Available online at www.sciencedirect.com
ScienceDirect
Journal of Theoretical Biology 243 (2006) 152–169
Journal of Theoretical Biology
www.elsevier.com/locate/yjtbi

Mathematical model of mitochondrial ionic homeostasis: Three modes of Ca^{2+} transport

Alexandra V. Pokhilko[a,c,*], Fazoil I. Ataullakhanov[a], Ekhson L. Holmuhamedov[b,d]

[a]*National Scientific Center for Hematology, Novozykovsky proezd 4a, Moscow 125167, Russian Federeation*
[b]*Mayo Clinic, Department of Cardiovascular Diseases, Rochester, MN 55905, USA*
[c]*Bioinformatics Institute, 30 Biopolis Street, #07-01, Matrix, Singapore 138671, Singapore*
[d]*University of North Carolina at Chapel Hill, 226 Taylor Hall, CB # 7090, Chapel Hill, NC 27599, USA*

Received 28 April 2006; received in revised form 30 May 2006; accepted 30 May 2006
Available online 7 June 2006

Abstract

Mitochondria play an important role in regulation of Ca^{2+} homeostasis in a cell. Here we present a mathematical model of mitochondrial ion transport and use this model to analyse different modes of Ca^{2+} uptake by mitochondria. The model includes transport of H^+, Ca^{2+}, K^+, inorganic phosphate and oxidative substrates across the inner mitochondrial membrane harboring permeability transition pore (PTP). The detailed description of ion fluxes is based on the experimental ion kinetics in isolated mitochondria. Using the model we show that the kinetics of Ca^{2+} uptake by mitochondria is regulated by the total amount of Ca^{2+} in the system and the rate of Ca^{2+} infusion. Varying these parameters we find three different modes of ion transport. When the total amount of Ca^{2+} is below 140 nmol Ca^{2+}/mg protein, all available Ca^{2+} is accumulated in the matrix without activation of the PTP. Between 140 and 160 nmol Ca^{2+}/mg protein, accumulation of Ca^{2+} generates periodic opening and closure of the PTP and oscillations of ion fluxes. Higher levels of Ca^{2+} (>160 nmol Ca^{2+}/mg protein) result in a permanently open PTP, membrane depolarization and loss of small ions from the matrix. We show that in the intermediate range of Ca^{2+} concentrations the rate of Ca^{2+} infusion regulates the PTP state, so that slow Ca^{2+} infusion does not lead to PTP opening, while fast Ca^{2+} infusion results in an oscillatory state.

Keywords: Mitochondria; PTP; Oscillation; Mathematical model; Ions transport

1. Introduction

Mitochondria are central to cellular physiology and fulfill multiple functions from ATP synthesis to modulation of intracellular Ca^{2+}, opening of the permeability transition pore (PTP) and release of factors initiating apoptotic cell death (Bernardi, 1999; Berridge et al., 2003; Duchen, 1999; Kroemer and Martin, 2005; Lemasters et al., 1999; McCormack and Denton, 1993; Parekh and Putney, 2005; Rudolf et al., 2004). Within the intracellular milieu, mitochondria are exposed to a continuously changing Ca^{2+} environment consisting of Ca^{2+} spikes, Ca^{2+} sparks and waves of free Ca^{2+} (Bowser et al., 2002; Hoth et al., 2000; Jouaville et al., 1995; Lin et al., 2005; Robb-Gaspers et al., 1998; Rudolf et al., 2004). It has been speculated that during a cell lifespan mitochondria could be rendered dysfunctional due to dangerous levels of accumulated Ca^{2+} (Bernardi, 1999; Berridge et al., 2003; Bowser et al., 2002; Duchen, 1999; Hoth et al., 2000; Lin et al., 2005; McCormack and Denton, 1993). However, mitochondria preserve their functions in cells for days, weeks and even months suggesting the existence of a defensive mechanism that allows the mitochondria to discharge excessive Ca^{2+} from the matrix and prevent Ca^{2+}-induced mitochondrial damage (Berridge et al., 2003; Bowser et al., 2002; Collins et al., 2002; Robb-Gaspers et al., 1998). Earlier observations showing that isolated mitochondria maintain energy-dependent ion flux oscillations (Carafoli et al., 1965;

*Corresponding author. Bioinformatics Institute, 30 Biopolis Street, #07-01, Matrix, Singapore 138671, Singapore. Tel.: +65 6478 8312; fax: +65 6478 9047.
E-mail addresses: apokhilko@yahoo.com (A.V. Pokhilko), fazly@hc.comcor.ru (F.I. Ataullakhanov), ekhson@med.unc.edu (E.L. Holmuhamedov).

0022-5193/$ - see front matter © 2006 Elsevier Ltd. All rights reserved.
doi:10.1016/j.jtbi.2006.05.025

Chance and Yoshioka, 1966; Evtodienko et al., 1980; Gooch and Packer, 1974; Graven et al., 1966; Holmuhamedov, 1986) allow us to hypothesize that mitochondrial oscillations might indeed also occur in vivo. These speculations have recently been confirmed by observations of mitochondrial membrane potential oscillations and the cyclic uptake and release of Ca^{2+} in mitochondria in vivo (Buckman and Reynolds, 2001; Fuller and Arriaga, 2003; Huser and Blatter, 1999; Monteith and Blaustein, 1999). Although there is a limited number of mathematical models of mitochondrial Ca^{2+} homeostasis (Cortassa et al., 2003; Magnus and Keizer, 1997, 1998; Selivanov et al., 1998), a mathematical model, that quantitatively describes the experimental data on the measured ion fluxes during Ca^{2+} uptake by mitochondria has not been presented.

Our goal is to build a model of mitochondrial ion transport that is based on the experimental ion kinetics and use this model to analyse different modes of Ca^{2+} uptake by mitochondria. To achieve this goal we incorporated the existing approaches to theoretical description of ion fluxes (Garlid et al., 1989; Magnus and Keizer, 1997) and modified them, when it was necessary for the better correspondence with experimental data (Model description and Appendix A). We also included into our model the main important processes, which were not included into the previous models, such as K^+ transport and matrix volume changes and the binding of matrix Ca^{2+} by immobile (matrix phospholipids) and mobile (substrate anions) buffers. The description of PTP was based on our previous model (Selivanov et al., 1998) with the following improvements. In our previous model, (Selivanov et al., 1998) we hypothesized that Ca^{2+} uptake results in an increase of matrix pH, which in turn leads to the PTP opening and loss of a hypothetical activator of mitochondrial respiration. This leak of the activator results in collapse of matrix pH and closure of the PTP. In our present model we describe mitochondrial oscillations without assuming the existence of a respiration activator that drives the oscillations. The oscillatory regime in our present model is a consequence of experimentally shown dependence of PTP on Ca^{2+} and mitochondrial membrane potential (Petronilli et al., 1993).

We use our model to investigate possible modes of Ca^{2+} uptake by mitochondria. We find that the modes are regulated by the amount of applied Ca^{2+} and by the rate of Ca^{2+} infusion. Our description of the mitochondrial responses to different levels of extra-mitochondrial Ca^{2+} and to different temporary dynamics of the outside Ca^{2+} can be useful for the quantitative predictions of mitochondria behavior in a cell. This is the first mathematical model of Ca^{2+} transport in mitochondria that includes the main components of mitochondrial ion transport and is in a good agreement with the existing experimental data.

2. Model description

Ion fluxes across the inner mitochondrial membrane used in our mathematical model are shown in Fig. 1. The energy of substrate oxidation in the mitochondrial matrix is transformed via a respiratory chain into the energy of an electrochemical gradient of hydrogen ions ($\Delta\mu H$) (Mitchell, 1972). The $\Delta\mu H$ that is stored in the form of electrical ($\Delta\Psi$) and concentration (ΔH) gradients provides the main driving force for the ion transport in mitochondria (Fig. 1). Our model consists of 5 individual modules (Modules #1–5 of Appendix A) that describe fluxes of the ions as well as the status of mitochondrial PTP.

Following is a brief description of the ionic fluxes in our model, while the detailed mathematical equations of each flux (Modules #1–5) as well as the complete model are given in the Appendix A.

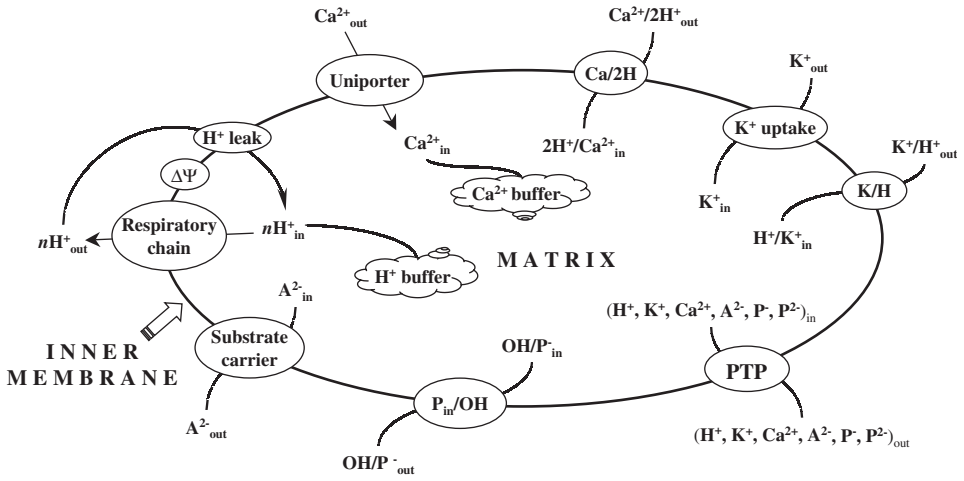

Fig. 1. The diagram of ion fluxes through the inner mitochondrial membrane. The model includes H^+ efflux through the respiration chain; H^+ passive influx (H^+ leak); Ca^{2+} fluxes through Ca^{2+} uniport and Ca/2H exchanger; K^+ fluxes through K^+ uniport and K/H exchanger; inorganic phosphate (P^-) flux through P/OH exchanger; substrate anion (A^{2-}) flux through dicarboxylic acid exchaner and the fluxes of all ions and Ca^{2+} complexes with anions (Ca–A, Ca–P) through open PTP. The model includes H^+ and Ca^{2+} binding with matrix buffers.

Module # 1. Mitochondrial proton transport: Mitochondria transport protons via: Respiratory chain; passive "leak" (H^+ leak); counter-fluxes of H^+ and Ca^{2+}, K^+, and phosphate (P^-) (Ca/2H, K/H, P/OH); and PTP.

Module # 2. Mitochondrial calcium transport: Mitochondrial Ca^{2+} transport: Ca^{2+} uniporter, $Ca^{2+}/2H^+$ exchanger (Ca/2H) and PTP.

Module # 3. Mitochondrial potassium transport: Mitochondrial K^+ transport: K^+ uniporter, K^+/H^+ exchanger (K/H), and PTP.

Module # 4. Mitochondrial anion transport: Mitochondrial anion transport: phosphate transport via P/OH and dicarboxylic acid A^{2-} (oxidative substrate) transport by its exchange with matrix phosphate P^{2-} (Dicarboxylate exchanger) and anions transport via PTP.

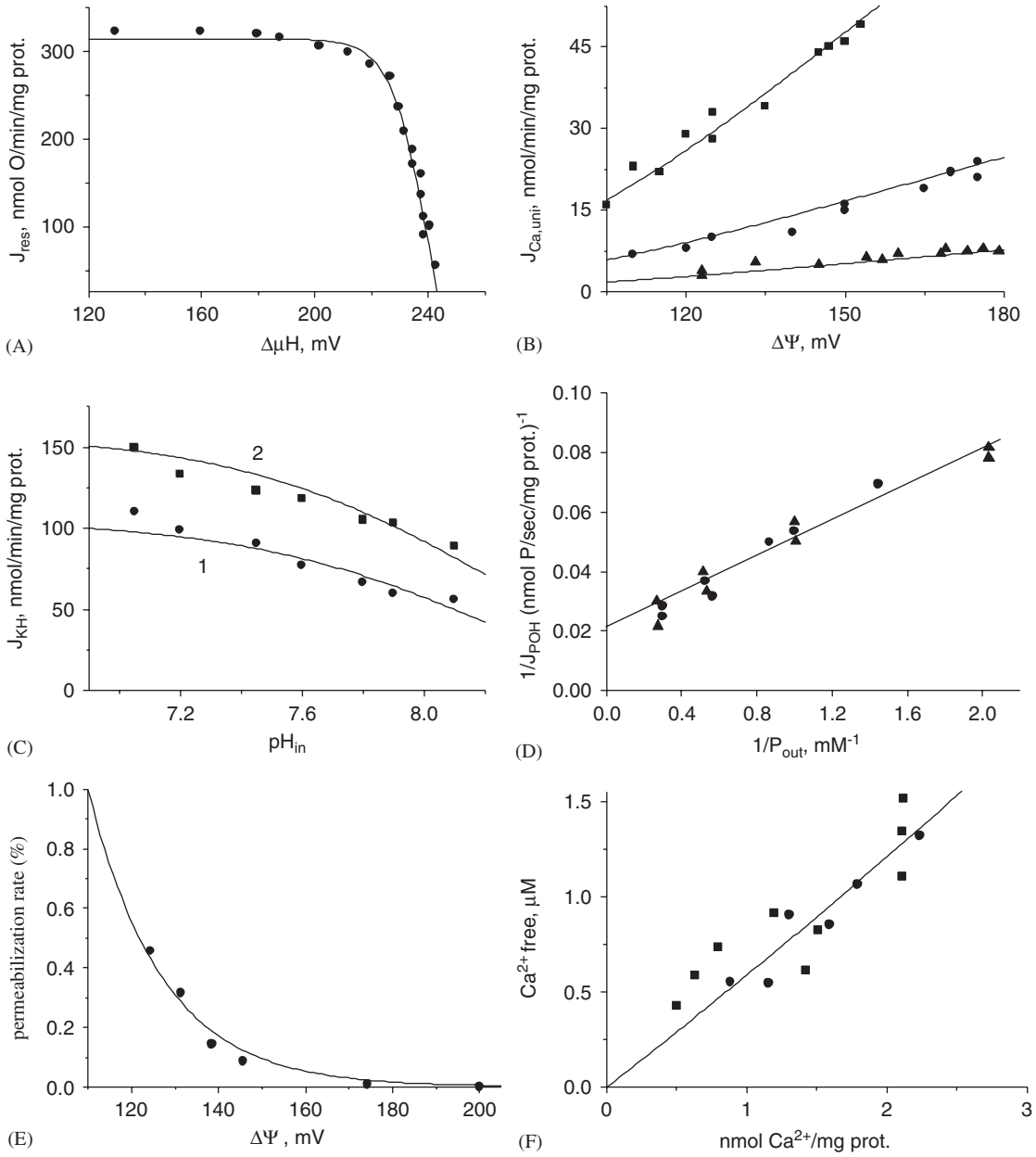

Fig. 2. Approximation of the experimental kinetics of ion fluxes (panels A–E) and Ca^{2+} buffering capacity of the matrix (panel F) by model equations, which are given in Appendix A. Experimental point are shown by symbols and model approximation by lines. (A) Dependence of the respiration rate on $\Delta\mu H$. (B) Dependence of the Ca^{2+} uniport rate on the membrane potential for three Ca^{2+} outside concentrations: 0.5, 0.9, 1.55 μM and $K_m^{uni} = 6.4$ mM. (C) Dependence of the rate of K^+/H^+ exchanger on extramitochondrial pH for two K^+ outside concentrations: 15 mM (1) and 30 mM (2). (D) Dependence of the rate of P/OH exchanger on the phosphate outside concentration for $pH_{out} = 7.2$. (E) Dependence of the PTP opening rate on $\Delta\Psi$. Experimental points were taken from (Doussiere et al., 1984; Wingrove et al., 1984; Brierley and Jung, 1990; Ligeti et al., 1985; Petronilli et al., 1993; Hansford and Castro, 1982) for the panels A–F correspondingly. (F) Dependence of the free matrix Ca^{2+} on the total matrix Ca^{2+} content. Model approximation with Eq. (16) is shown by line.

Module # 5. Mitochondrial permeability transition pore: This module describes the regulation of PTP status with matrix Ca^{2+}, H^{+} and membrane potential and fluxes of ions via PTP.

We used the existing theoretical approaches for description of ion flux kinetics (see Appendix A). In some cases we improved the existing formulae to achieve the best correspondence of the model with the experimental data (for Respiratory chain, Ca^{2+} uniporter, K/H and P/OH exchangers, PTP). Fig. 2A–E shows that the formulae we developed describe well the experimental data for the measured mitochondrial characteristics. We also included into the model both fixed and mobile Ca^{2+} anion buffers in matrix (Appendix A). The derived dependence of the matrix free Ca^{2+} concentration on the total matrix Ca^{2+} content corresponds well with the experimental data (Fig. 2F).

The individual flux equations were combined with the model of ion transport and are described by a system of ordinary differential equations (ODEs) (Eq. (14), Appendix A). We next compared the model results with the experimental data on the kinetics of pH and Ca^{2+} in isolated mitochondria. Fig. 3A shows, that the model describes well the measured kinetic of matrix pH after addition of phosphate into the medium (Jung et al., 1989). The model simulations of our experiments on Ca^{2+} uptake by mitochondria (Holmuhamedov et al., 1999) are shown on Fig. 3B. These experiments were done in the presence and in the absence of the PTP inhibitor (cyclosporin A) and diazoxide. Diazoxide at this high concentration is a powerful uncoupler (Kowaltowski et al., 2001). To simulate the diazoxide effects we increased the mitochondrial permeability to H^{+} (see Fig. 3B). Cyclosporin A influence was modeled by switching off PTP opening. As it is seen from Fig. 3B, our model describes well the kinetics of Ca^{2+} uptake with and without opening of PTP.

We used the model to analyse different regimes of Ca^{2+} uptake by mitochondria (Section 3). Ion concentrations in the matrix and incubation medium were the *variables*, while the total ion content in the mitochondrial matrix and medium were the *parameters* of our model. In the calculations shown in Section 3 we varied the total amount of Ca^{2+}, while keeping other parameters constant as described in the figure legends. The system of ODEs (14) was analysed using DBSOLVE software (Goryanin et al., 1999) with LSODA method (Hindmarsh, 1980).

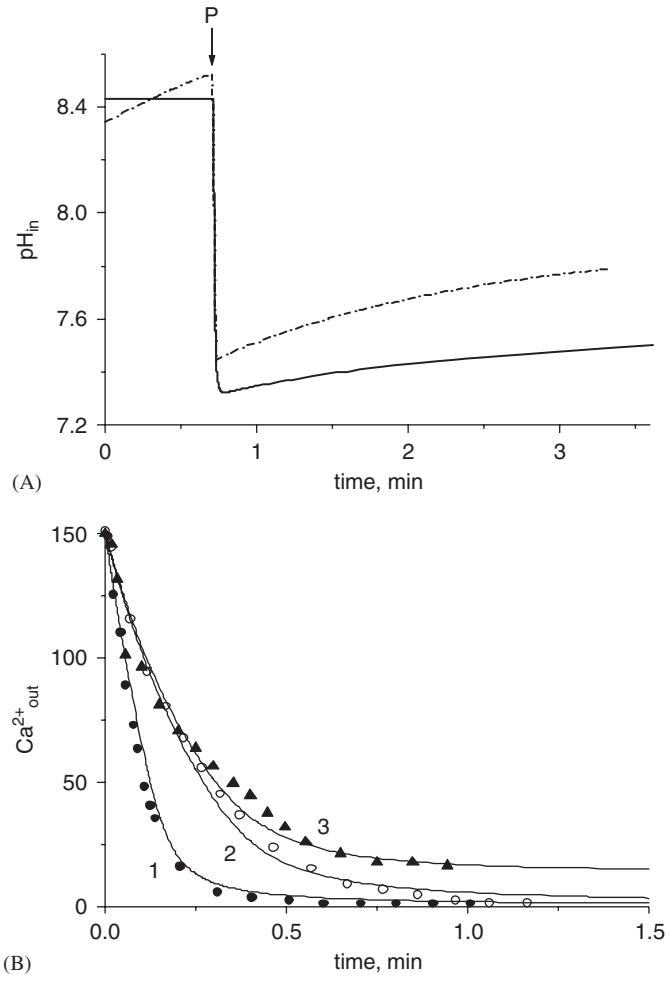

Fig. 3. Comparison of experimental and model pH and Ca^{2+} kinetics for isolated mitochondria. (A) Matrix pH changes after an addition of phosphate (2 mM) into the medium. The medium contained: 100 mM K^{+}, 0 mM phosphate, 4 mM succinate, 0.5 mg prot./ml, pH = 7.2. Phosphate (P) addition is shown by an arrow. Experimental kinetics (dash line) was taken from (Jung et al., 1989), model approximation is shown by solid line. (B) The kinetics of Ca^{2+} uptake by mitochondria. Experimental points were taken from (Holmuhamedov et al., 1999). The model results are shown by lines: 1—without diazoxide, 2—with diazoxide (300 μM) and cyclosporin A (2 μM), 3—with diazoxide (300 μM) and without cyclosporin A. The values of diazoxide-induced H^{+} permeability $P_{H,\ leak}$ was taken as 140 ml/mg/min. The PTP was considered to be closed in presence of cyclosporin A. Incubation medium contained: 150 μM Ca^{2+}, 110 mM K^{+}, 5 mM phosphate, 5 mM malate, 1 mg prot./ml, pH = 7.3.

3. Results

Numerical simulation of our mathematical model demonstrated the existence of three distinct inter-convertible modes of mitochondrial ion transport. Transitions between these modes are determined by the status of the Ca^{2+}-sensitive PTP. The large assortment of ion transport patterns generated through numerical simulation of the model is presented below.

3.1. Mitochondrial ion transport at low Ca^{2+} loading

The kinetics of mitochondrial variables after addition of 100 μM Ca^{2+} into the mitochondrial suspension is shown in Fig. 4. The initial phase of Ca^{2+} uptake was associated with a rapid increase in matrix Ca^{2+} (Fig. 4A) and moderate alkalization of the mitochondrial matrix (Fig. 4B) due to the extrusion of matrix H^{+} in exchange for transported Ca^{2+}. Extruded H^{+} ions are returned into the matrix via H^{+}-leak, K^{+}/H^{+} exchanger and co-transport of H^{+} with phosphate (Fig. 4B). During Ca^{2+} uptake, the

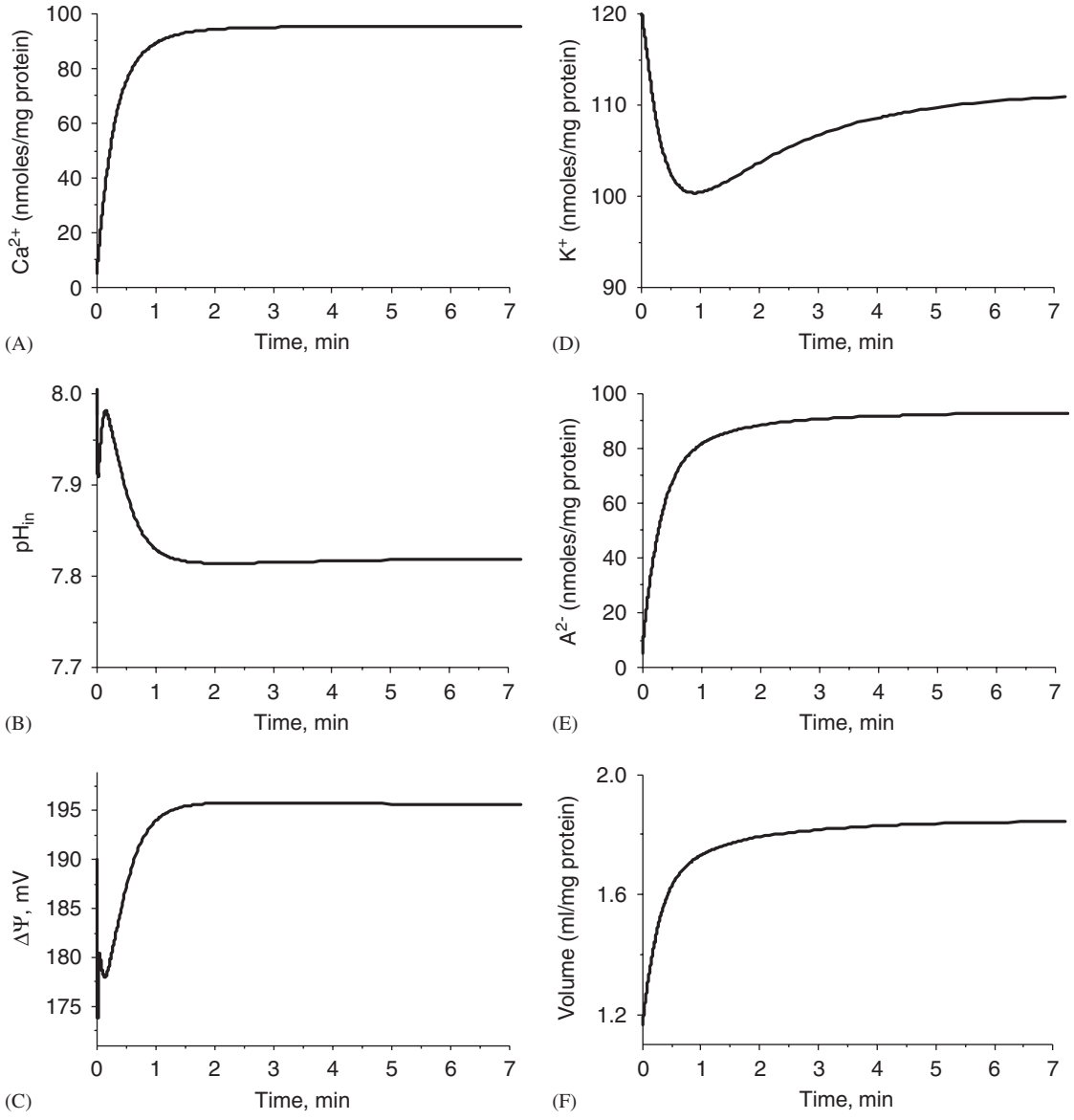

Fig. 4. The kinetics of matrix Ca^{2+} (A), pH (B) and membrane potential (C) following exposure of mitochondria to step-wise jump in Ca^{2+} concentration (100 μM). Shown also are the changes in the matrix content of K^+ (D), anions A^{2-} (E) and the matrix volume (F). Incubation medium contained: 100 mM K^+, 0.3 mM phosphate (P), 5 mM malate (A^{2-}), 1 mg prot./ml, pH = 7.4. At the zero time-point 100 μM Ca^{2+} was added to suspension and all changes were calculated using the system of ODEs (14). Initial conditions: $\Delta\Psi = 190$ mV, $pH_{in} = 8$, $T_{op} = 0$, total matrix content of Ca^{2+} (5 nmol/mg prot.), K^+ (120 nmol/mg prot.), phosphate and malate (5 nmol/mg prot. each), NAD^+ (2 nmol/mg prot.).

mitochondrial membrane potential undergoes transient depolarization (Fig. 4C), reflecting the initial high rate of Ca^{2+} influx, which slowed at later stages due to reduced extra-mitochondrial Ca^{2+} concentration (Fig. 4A). The transient changes in membrane potential and matrix pH (Fig. 4B and C) are translated into the fall and elevation of K^+ concentrations in the matrix mediated by K^+ uniporter and K^+/H^+ exchanger (Fig. 4D). The steady accumulation of anions in the mitochondrial matrix (Fig. 4E) results in mitochondrial swelling and increased matrix volume (Fig. 4F).

Further analysis of the model shows that at each level of Ca^{2+} loading up to 140 nmol Ca^{2+}/mg prot., the model demonstrated existence of the only stable steady state, which is characterized by closed PTP and accumulation of ions in the matrix.

3.2. Mitochondrial ion transport at intermediate Ca^{2+} loading

Increase in the total Ca^{2+} loading results in a change of the mode of mitochondrial ion transport from a steady-state ion uptake into a mode of repetitive uptake and release of ions by the mitochondria. The typical oscillations of mitochondrial variables are shown in Fig. 5. These oscillations appear when the Ca^{2+} load of mitochondria

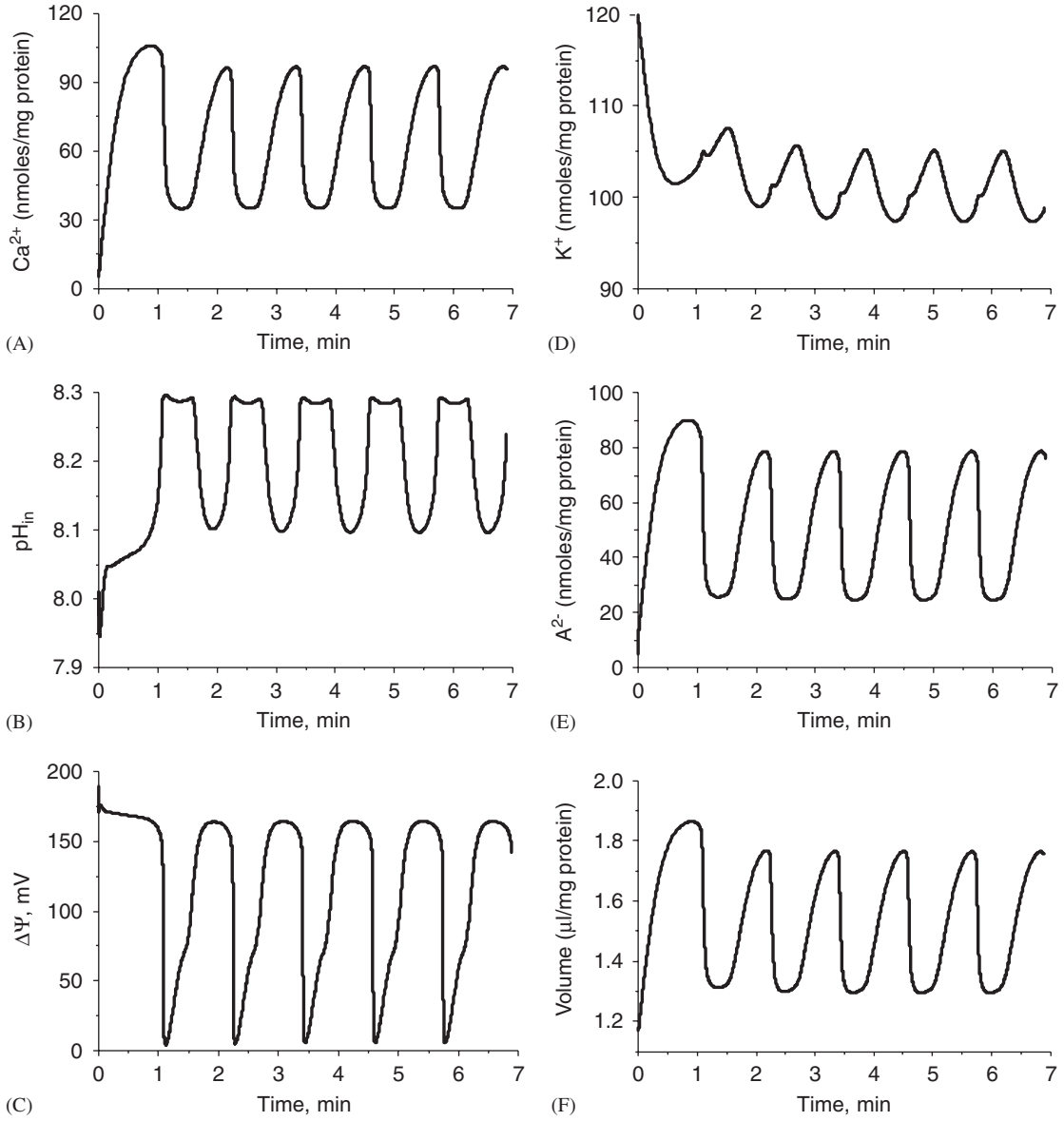

Fig. 5. Numerical simulation of the oscillations of matrix Ca^{2+} (A), pH (B), membrane potential (C), matrix K^+ (D), anions A^{2-} (E) and the matrix volume (F). At zero time-point mitochondria were exposed to 140 μM Ca^{2+}. Incubation medium and initial conditions are described in Fig. 4 legend.

falls within the range between 140 and 160 nmol Ca^{2+}/mg prot. The initial Ca^{2+} uptake followed by membrane depolarization and alkalization of the matrix promotes opening of the mitochondrial PTP (Eq. (10), Appendix A) resulting in an efflux and redistribution of ions such as Ca^{2+}, K^+, A^{2-} and an influx of H^+.

The efflux of Ca^{2+} and influx of H^+ leads to the changes in their matrix concentrations to a level insufficient to maintain open state of the PTP resulting in the pore closing (Eq. (10), Appendix A). Closure of the PTP and restoration of the initial low membrane permeability allows the mitochondrial respiratory chain to rebuild membrane potential and initiate the next cycle of energy-dependent Ca^{2+} uptake, which results in opening of the PTP and in turn generation of the oscillations (Fig. 5).

It is important to note that mitochondrial ion transport at intermediate Ca^{2+} loading demonstrates co-existence of two modes of mitochondrial ion transport: (i) oscillation state and (ii) stable steady state. Depends on the initial ion concentrations; the mitochondria enter one of the two states, thus demonstrating the bistable behavior of the system at intermediate Ca^{2+} load. As shown in the Section 3.4, the mode of mitochondrial ion transport at these Ca^{2+} load can be regulated by the rate of Ca^{2+} infusion into the medium.

3.3. Mitochondrial ion transport at high Ca^{2+} loading

Further increase in the Ca^{2+} loading (above 160 nmol Ca^{2+}/mg prot.) results in a new mode of ion transport, which is characterized by a permanently open PTP (Fig. 6).

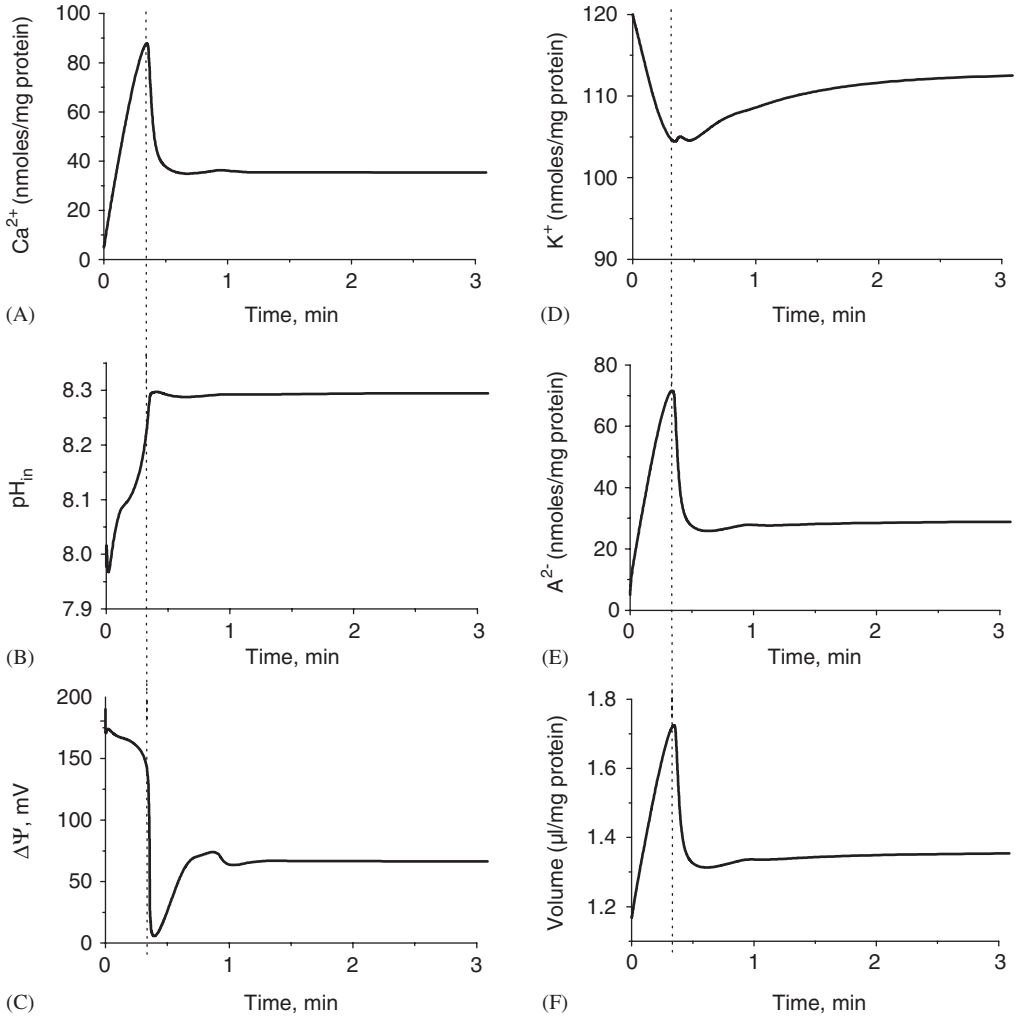

Fig. 6. Numerical simulation of mitochondrial ion transport upon high Ca^{2+} loading. At zero time-point mitochondria were exposed to 200 μM Ca^{2+}. Incubation medium and initial conditions are described in Fig. 4 legend.

Increase of matrix Ca^{2+} and pH lead to PTP opening followed by the efflux of Ca^{2+} and influx of H^+ within the matrix thus creating conditions that should close PTP and "reseal" the inner membrane. However, due to a large amount of total Ca^{2+} present in the suspension, the matrix Ca^{2+} never drops below the activation threshold of the PTP, leaving it permanently open. This "point-of-no-return" for the mitochondrial ion transport under excessive Ca^{2+} loading is represented in Fig. 6 by a dashed vertical line. Model analysis shown, that at all Ca^{2+} loads above 160 nmol Ca^{2+}/mg prot. mitochondria demonstrate only one stable steady state with an open PTP.

The analysis of our model is in a good agreement with earlier experimental observations that the mode of ion transport is determined by the total Ca^{2+} loading (Evtodienko et al., 1980; Holmuhamedov, 1986; Magnus and Keizer, 1997, 1998; Selivanov et al., 1998). The dependence of the ion transport mode on the Ca^{2+} loading is illustrated in Fig. 7. This diagram shows the steady-state matrix Ca^{2+} contents at different Ca^{2+} loads. Line 1 corresponds to the "low" Ca^{2+} loads with closed PTP, dash lines 2 indicate the oscillation range for the "intermediate" Ca loads and line 3 corresponds to the "high" Ca^{2+} loads with opened PTP.

3.4. *Mitochondrial ion transport at Ca^{2+} loading by infusion*

Although the mode of ion transport is determined by the total Ca^{2+} load, analysis of the ion fluxes in mitochondria revealed that the ion transport mode at the intermediate Ca^{2+} loads is also dependent on the rate of Ca^{2+} infusion into the system.

Throughout this article we have demonstrated the effect of stepwise increase in matrix Ca^{2+} concentration in the incubation medium on mitochondrial ion transport. However, the same level of Ca^{2+} can be achieved by a continuous infusion of Ca^{2+} into the respiring suspension. Analysis of the ion transport at different rates of Ca^{2+} infusion demonstrated the existence of a threshold rate, which differentiates between the steady ion transport mode

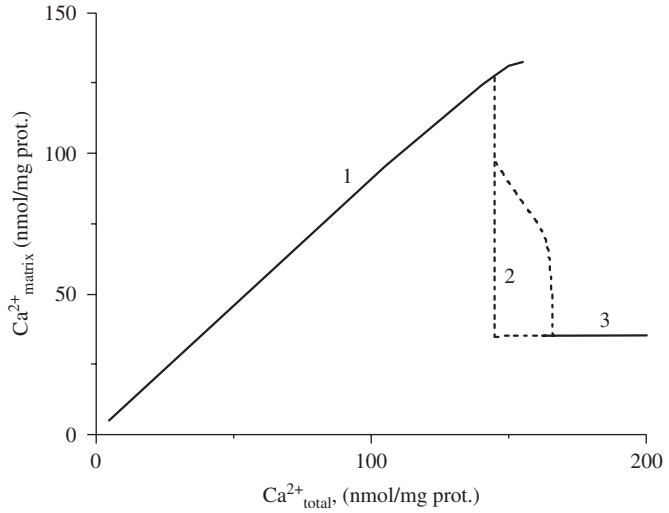

Fig. 7. Dependence of the steady-state matrix Ca^{2+} on the total amount of Ca^{2+} loading into the mitochondria. The line 1 corresponds to the "low" Ca^{2+} loads with closed PTP; the dashed lines 2 indicate the oscillation range for the "intermediate" Ca^{2+} loads and the line 3 corresponds to the "high" Ca^{2+} loads with opened PTP. Incubation medium is described in Fig. 4 legend.

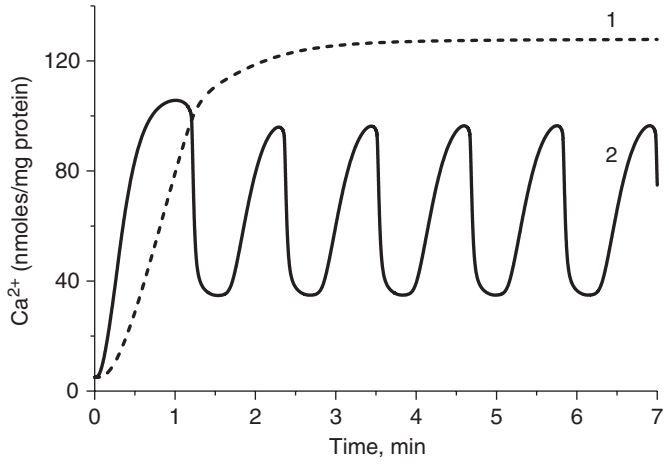

Fig. 8. Numerical simulation of the time-course of the matrix Ca^{2+} concentration obtained at two different rates of Ca^{2+} infusion. *Curves* 1 or 2 correspond to the rate of Ca^{2+} infusion 2 or 8 nmol Ca^{2+}/s/mg prot., respectively. Incubation medium and initial conditions are described in Fig. 4 legend.

and oscillatory mode. The value of this critical infusion rate depends on Ca^{2+} load and for those presented in Fig. 5 the critical rate of Ca^{2+} infusion is 4.1 nmol/mg prot./s. If the rate of Ca^{2+} infusion is below critical, the PTP remains closed. However, if the rate of Ca^{2+} infusion is above the critical, the system enters oscillatory state as illustrated in Fig. 8. Curve 1 was obtained with the infusion rate 2 nmol Ca^{2+}/mg/s, when PTP remains closed and all Ca^{2+} is accumulated into the matrix; whereas curve 2 was obtained with the infusion rate 8 nmol Ca^{2+}/mg/s (Fig. 8), when ion transport enters the oscillatory mode. Our model prediction about the dependence of the ion transport mode on the rate of Ca^{2+} infusion is consistent with the experimental data on Ca^{2+} oscillations in mitochondria (Holmuhamedov et al., 1995; Ichas et al., 1994).

4. Discussion

Here we present the mathematical model of mitochondrial ion transport, which is based on experimental data on isolated mitochondria. The model describes the transport of H^+, Ca^{2+}, K^+, anions, and the regulation of PTP. Since our goal was to describe the ion transport processes, we did not consider the synthesis of ATP in our model. We predict that depending on the extra-mitochondrial amount of Ca^{2+}, mitochondria enter one of three modes of Ca^{2+} transport: **1**—Ca^{2+} accumulation (low Ca^{2+} load, Fig. 4), **2**—Ca^{2+} oscillation (intermediate Ca^{2+} load, Fig. 5) and **3**—Ca^{2+} release (high Ca^{2+} load, Fig. 6). These modes are characterized by different state of PTP: closed, periodically opened and permanently opened. Further analysis also demonstrated that, at a level of intermediate Ca^{2+} loading, the rate of Ca^{2+} infusion into the mitochondrial suspension determines the mode of ion transport (Fig. 8). Our model predicts the existence of a critical rate of Ca^{2+} infusion, above which the steady state is replaced by the oscillatory state (Fig. 8). The mechanistic explanation of this observation is that the faster rates of Ca^{2+} loading decrease the membrane potential, thus promoting the opening of PTP. This result agrees well with experimental data on isolated rat liver mitochondria exposed to Sr^{2+} (Ca^{2+}) ions (Holmuhamedov et al., 1995).

It is interesting to consider possible implications of our results in the cellular context. Mitochondria are known to be active participants in Ca^{2+} cellular hemostasis. However, for a long time it was not clear, how low-affinity Ca^{2+} uniporter can result in fast Ca^{2+} accumulation by mitochondria from the bulk cytoplasm, which contains only several μM of free Ca^{2+} (Rizzuto and Pozzan, 2006; Herrington et al., 1996; Hoth et al., 1997). Modern data clearly demonstrate that Ca^{2+} uptake by mitochondria is highly spatially in-homogeneous. Although mitochondria can slowly accumulate Ca^{2+} from bulk cytoplasm, the efficient accumulation of Ca^{2+} occurs only in microdomains of high Ca^{2+} (see Rizzuto and Pozzan, 2006 for review). Local Ca^{2+} concentration measured in these microdomains reaches the level of several hundred μM (Rizzuto and Pozzan, 2006), which is comparable with the Ca^{2+} concentrations used in the experiments on isolated mitochondria. These high Ca^{2+} concentrations can provide fast Ca^{2+} accumulation by mitochondria through the Ca^{2+} uniporter. It was shown that Ca^{2+}, which first is absorbed by mitochondria at discrete number of sites then rapidly diffuses through the mitochondrial network (Rizzuto and Pozzan, 2006). This diffusion disperses Ca^{2+} concentration in mitochondria, so that under normal condition mitochondria can accumulate large amount of

Ca^{2+} without the opening of PTP and subsequent drop of mitochondrial membrane potential (Eriksson et al., 1999).

Mitochondrial Ca^{2+} buffer is another important factor, which allows mitochondria to retain high amounts of Ca^{2+} without significant rise in the matrix free Ca^{2+} concentration. In our model we took into consideration a very large Ca^{2+} buffering capacity of mitochondria that allows them to accumulate Ca^{2+} to the level sufficient for activation of matrix enzymes, but below PTP activation level (Coll et al., 1982). The model simulations show that mitochondria can accumulate up to 140 nmol Ca^{2+}/mg protein without the opening of PTP, which corresponds to normal physiological conditions in a cell in the microdomains zone (the low Ca^{2+} mode in our model). However, under conditions of higher Ca^{2+} loading, the Ca^{2+} buffer capacity of the matrix becomes exhausted and favors the PTP opening, which corresponds to the Ca^{2+} overloading conditions in a cell.

The role of mitochondria in the total and complex oscillatory Ca^{2+} dynamics in a cell was considered in a number of mathematical models (Falcke et al., 1999; Marhl et al., 2000; Meyer and Stryer, 1988). It was shown (Marhl et al., 2000) that fast Ca^{2+} uptake and slow Ca^{2+} release by mitochondria allows to describe well the experimental data on the Ca^{2+} dynamics in a cell under conditions, which are not accompanied by drop in mitochondrial membrane potential as a result of opening PTP (Eriksson et al., 1999). However, under conditions of Ca^{2+} overloading and oxidative stress, some mitochondria demonstrate oscillations of membrane potential and Ca^{2+} concentration, which result from short-term opening of PTP (Huser and Blatter, 1999; Monteith and Blaustein, 1999). Possibly, this depolarization of mitochondrial membrane first occurs in Ca^{2+} microdomains and then spreads along the mitochondrial network. Our model describes this experimental phenomenon of mitochondrial PTP oscillations under conditions, when the extra-mitochondrial Ca^{2+} rises above the critical level. In vivo these oscillations can save Ca^{2+}—overloaded mitochondria from the permanent PTP opening, allowing the excessive extra-mitochondria Ca^{2+} to diffuse into the cytoplasm. Our simulations show, that mitochondrial ion transport modes depend not only on the cytoplasmic Ca^{2+} level, but also on the rate of Ca^{2+} influx into the system.

The incorporation of our mathematical model of mitochondrial Ca^{2+} transport into the general model of Ca^{2+} cellular hemostasis can help to describe the complex spatial Ca^{2+} dynamics in a cell under conditions favoring the PTP opening, such as ischemia, Ca^{2+} overloading and oxidative stress.

Acknowledgments

We thank Dr. V.A. Selinvanov, Prof. L.S. Yaguzhinsky and A. Dubrovskii for their suggestions and insights, and Holmuhamedov A. for his contribution in editing the manuscript. Special thanks go to Dr. A.B. Goryachev for critical reading of manuscript and providing valuable contribution into the improvement of a style of the paper. This study was supported in part by a grant from Russian Foundation for Basic Research, Project No. 03-04-48338 (F.I.A.).

Appendix A

The model consisted of five blocks, describing the kinetics of the H^+, Ca^{2+}, K^+, P^-, A^{2-} ion fluxes and the status of the PTP with the constants of the model given in Table 1.

Table 1
Constants of the model

Constant	Value	References
Module#1. H^+ transport		
Respiration-driven outward H^+ ejection		
Matrix $NADH_t$+NAD_t (nmol/mg prot.)	8	Magnus and Keizer (1997)
K_2	5.37×10^{15}	Magnus and Keizer (1997)
K_3	1.2×10^{13}	Magnus and Keizer (1997)
K_4	3.41×10^{13}	Magnus and Keizer (1997)
K_5	0.17	Magnus and Keizer (1997)
K_6	1.42	Magnus and Keizer (1997)
$H^+/NADH$ ratio	12	Magnus and Keizer (1997)
k_m^H (mM)	10^{-5}	Kauffman and Lardy (1980)
K_1 (nmol/min/mg prot.)	21.6	Doussiere et al. (1984)
g	0.64	Doussiere et al. (1984)
K_{NADH} (μl/min/mg prot.)	100	Erecinska and Wilson (1982)
Back-flow of extruded H^+ ions		
β	1	Brown and Brand (1986)
$P_{H,leak}$ (ml/min/mg prot.)	0.39	Brown and Brand (1986)

Table 1 (*continued*)

Constant	Value	References
pH-buffering capacity of the mitochondrial matrix		
B_H (nmol/mg prot.)	50	Mitchell and Moyle (1969)
K_H^b (mM)	3×10^{-5}	Mitchell and Moyle (1969)
F/RT	0.039	Magnus and Keizer (1997)
Module#2. Ca^{2+} transport		
Ca^{2+} uptake		
P_{uni} (nmol/min/mg prot.)	38.5	Gunter and Pfeiffer (1990), Evtodienko et al. (1980)
K_m^{uni} (mM)	0.07	Gunter and Pfeiffer (1990)
$\Psi_0{}^{uni}$ (mV)	13	Wingrove et al. (1984)
$\Psi_1{}^{uni}$ (mV)	124	Wingrove et al. (1984)
Ca^{2+} efflux		
$V_{\max}^{CaH}$ (nmol/min/mg prot.)	1.2	Wingrove and Gunter (1986)
k_m^{CaH} (mM)	0.0084	Wingrove and Gunter (1986)
Intramitochondrial Ca^{2+} binding		
k_d^{Ca-PL} (mM)	0.023	Scarpa and Azzi (1968)
$PL_t{}^0$ (nmol/mg prot.)	40	Scarpa and Azzi (1968)
k_d^{Ca-A} (mM)	3	Martell (1964)
k_d^{Ca-P} (mM)	3	Martell (1964)
Module#3. K^+ transport		
K uptake		
P_K (μl/min/mg prot.)	0.03	Kowaltowski et al. (2001), Belyaeva and Wojtczak (1994)
β_K	0.25	Paucek et al. (1992)
K^+ efflux		
$V_{\max}^{KH}$ (nmol/min/mg prot)	600	Brierley and Jung (1990)
K_K (mM)	40	Brierley and Jung (1990)
K_H (mM)	1×10^{-5}	Brierley and Jung (1990)
Module#4. Anion transport		
Electroneutral P/OH exchanger		
K_P (mM)	1	Ligeti et al. (1985)
K_{OH} (mM)	2×10^{-4}	Ligeti et al. (1985)
$V_{\max}^{POH}$ (nmol/min/mg prot.)	21 000	Ligeti et al. (1985), Ataullakhanov et al. (1978)
P^- dissociation		
k_d^P (mM)	6×10^{-5}	Martell (1964)
Transport of oxidative substrates		
$V_{\max}^{dic}$ (nmol/min/mg prot.)	21,000	Indiveri et al. (1989), Ligeti et al. (1985)
K_P^{dic} (mM)	1.4	Tyler and Sutton (1984)
K_A (mM)	0.5	Tyler and Sutton (1984)
Module#5. PTP		
k_m^{PTP} (mM)	3.2×10^{-5}	Szabo et al. (1992)
Ψ_0 (mV)	110	Petronilli et al. (1993)
Ψ_1 (mV)	20	Petronilli et al. (1993)
k_{op} (min^{-1})	2	Evtodienko et al. (1980)
k_{cl} (min^{-1})	100	Evtodienko et al. (1980)
Ψ_2 (mV)	70	Evtodienko et al. (1980)
P_{PTP}^c (μl/min/mg prot.)	3	Evtodienko et al. (1980)
P_{PTP}^a (μl/min/mg prot.)	30	Evtodienko et al. (1980)
P_{PTP}^n (μl/min/mg prot.)	100	Evtodienko et al. (1980)
Membrane potential and matrix volume		
C_{mito} (nmol/mV/mg prot.)	1.45×10^{-3}	Magnus and Keizer (1997)
v_0 (μl/mg prot.)	0.28	Beavis et al. (1985)
S_0 (nmol/mg prot.)	87	Beavis et al. (1985)
F (mOsm/l)	275	Beavis et al. (1985)

A.1. Module #1. Mitochondrial proton transport

A.1.1. Respiration-driven outward H^+ ejection

We adopted an approach developed by Keizer and colleagues (Magnus and Keizer, 1997; Magnus and Keizer, 1998; Pietrobon and Caplan, 1985) for the description of NADH-dependent H^+ pumps (Bernardi, 1999; Duchen, 1999). Since the accumulation of large amounts of Ca^{2+} within the mitochondria is associated with significant changes in the matrix pH (Chance, 1965; Nicholls and Akerman, 1982), we took into account the inhibition of the H^+ pump activity by matrix H^+ (Chance, 1965; Kauffman and Lardy, 1980; Nicholls and Akerman, 1982). Ejection of H^+ was considered to be proportional to the rate of NADH oxidation (Holzhutter et al., 1985; Magnus and Keizer, 1997; Magnus and Keizer, 1998) and the rate of NADH replenishment (J_{NADH}) was defined as $J_{NADH} = -K_{NADH}\,NAD$, where NAD is the NAD^+ concentration in the matrix and K_{NADH} is the equilibrium constant of the matrix NADH-dehydrogenase defined from the experimental observation of the NADH/NAD ratio in the state 4 (Erecinska and Wilson, 1982; Magnus and Keizer, 1997; Magnus and Keizer, 1998). The resulting equation for the rate of respiration-driven ejection of H^+ ions from the matrix is given as follows:

$$J_{H,res} = K_1 \frac{K_2\sqrt{\frac{NADH}{NAD}} - \exp(g6F\Delta\mu H/RT)}{K_3 + K_4\sqrt{\frac{NADH}{NAD}} + \left[K_5 + K_6\sqrt{\frac{NADH}{NAD}}\right]\exp(g6F\Delta\mu HRT)} \frac{H^+}{H^+ + k_m^H}. \quad (1)$$

Fig. 2A shows, that the formula (1) give good approximation of the dependence of the rate of oxygen consumption on $\Delta\mu H$ (Doussiere et al., 1984), with constants K_1 and g given in Table 1.

A.1.2. Back-flow of extruded H^+ ions

Protons tend to reenter the matrix via passive "leak" in the membrane that dissipates the energy of $\Delta\mu H$. This back-flow of H^+ ($J_{H,leak}$) has exponential dependence on the membrane potential (Brown and Brand, 1986). In our model we used Eyring approximation for the H^+ influx (Brown and Brand, 1986; Garlid et al., 1989):

$$J_{H,leak} = P_{H,leak}(H_{out}\exp(\beta F\Delta\Psi/RT) - H_{in}\exp(-(1-\beta)F\Delta\Psi/RT), \quad (2)$$

where H_{out}, H_{in} are extra- and intra-mitochondrial H^+ concentrations, and R, T, and F maintain their usual meaning. $P_{H,\ leak}$ is a permeability of the mitochondrial membrane for H^+. The values of $P_{H,\ leak}$ and β were defined from a fitting of the experimental data (Brown and Brand, 1986) to the Eq. (2) and given in Table 1.

A.1.3. Mitochondrial matrix pH

For accurate description of the matrix H^+ concentration we took into account binding of matrix H^+ to the matrix buffer B (Mitchell and Moyle, 1969). From the binding reaction $B + H^+ \Leftrightarrow BH$ we describe the free matrix H^+ concentration as a function of total proton content (H_t):

$$H^+ = \frac{H_t - B_H - K_H^b v + \sqrt{(H_t - B_H - K_H^b v)^2 + 4K_H^b v H_t}}{2v}, \quad (3)$$

where B_H is the total amount of H^+ binding sites in the matrix, and K_H^b is the dissociation constant. This equation with the constants given in Table 1 provides good approximation of experimental data on the matrix pH buffering capacity (Mitchell and Moyle, 1969).

A.2. Module#2. Mitochondrial calcium transport

A.2.1. Ca^{2+} uptake

Goldman's approximation of the constant electrical field has been frequently used to describe Ca^{2+} uptake via a mitochondrial Ca^{2+} uniporter (Magnus and Keizer, 1997, 1998; Selivanov et al., 1998). However, a fit of the available experimental data by Goldman's equation required a modification of the equation and postulation of a (–90 mV) negative shift within the pore of the uniporter (Magnus and Keizer, 1997, 1998; Wingrove et al., 1984). Here, we excluded this negative shift that failed to accurately predict any steady-state distribution of Ca^{2+} ions across the membrane (Gunter and Pfeiffer, 1990). We used a non-modified Goldman approximation to describe Ca^{2+} fluxes through the uniporter (J_{uni}):

$$J_{uni} = P(Ca_{out}, \Delta\Psi)2F\Delta\Psi/RT \times \frac{(Ca_{out} - Ca_{in}\exp(-2F\Delta\Psi/RT))}{(1 - \exp(-2F\Delta\Psi/RT))}, \quad (4)$$

where J_{uni} is the Ca^{2+} flux via a uniporter, $P(Ca_{out}, \Delta\Psi)$ is the permeability of the uniporter, and Ca_{out} and Ca_{in} are the extra and intra-mitochondrial free Ca^{2+} concentrations. The permeability of the uniporter $P(Ca_{out}, \Delta\Psi)$ is a function of the mitochondrial membrane potential (Kapus et al., 1991) and the extra-mitochondrial Ca^{2+} (Gunter and Pfeiffer, 1990), which can be approximated as follows:

$$P(Ca_{out}, \Delta\Psi) = f(Ca_{out})g(\Delta\Psi). \quad (4a)$$

The expression for $f(Ca_{out})$ was obtained using sigmoid dependence of the initial rate of Ca^{2+} uptake on the Ca_{out} (Magnus and Keizer, 1997; Gunter and Pfeiffer, 1990). Taking into account the negligible value of the exponential term in Goldman equation for J_{uni} ($\Delta\Psi > 100$ mV), $f(Ca_{out})$ can be expressed as follows:

$$f(Ca_{out}) = P_{uni}\, Ca_{out}/[(Ca_{out})2 + (K_m^{uni})^2], \quad (4b)$$

where P_{uni} is the maximum permeability of the Ca^{2+} uniporter and K_m^{uni} is a Michaelis's constant for the uniporter. For numerical simulation of Ca^{2+} fluxes in the mitochondria we used the following values for $K_m = 0.07$ mM and $P_{uni} = 38.5$ nmol/min/mg prot., which match the initial rate of Ca^{2+} uptake in experiments on the Ca^{2+} oscillations in mitochondria (Evtodienko et al., 1980).

The function ($g(\Delta\Psi)$) was approximated as follows:

$$g(\Delta\Psi) = (\Delta\Psi - \Psi_0^{uni})^3/[(\Psi_1^{uni})^3 + (\Delta\Psi - \Psi_0^{uni})^3], \quad (4c)$$

where the constants Ψ_0 and Ψ_1 were determined from the experimental data (Wingrove et al., 1984) on the dependence of the uniporter rate on the membrane potential ($\Psi_0^{uni} = 13$ mV, $\Psi_1^{uni} = 124$ mV). Fig. 2B shows that with these constants the model describes well the experimentally observed dependence of the rate of the Ca^{2+} uniporter on the membrane potential.

A.2.2. Ca^{2+} efflux

Accumulated Ca^{2+} may be released from mitochondria either upon membrane depolarization and reversal of the Ca^{2+} uniporter, or through an electro-neutral exchange pathway, such as Ca/2Na or Ca/2H (Bernardi, 1999; Duchen, 1999; Gunter et al., 2004; Wingrove et al., 1984). Since the mitochondrial ion flux oscillations were observed in a nominally Na^+ free medium (Graven et al., 1966), here(Evtodienko et al., 1980; Gooch and Packer, 1974; Holmuhamedov, 1986; Tashmukhamedov and Gagel'gans, 1970) we considered an electro-neutral Ca/2H exchanger as the main electro-nutral efflux of Ca^{2+}, which is correct for mitochondria from some tissues like heart tissue (Wingrove and Gunter, 1986). As shown our preliminary calculations, the observed three modes of Ca^{2+} uptake also exist in the model with Ca/2Na exchanger (described by the equation defined in Magnus and Keizer (1997)), which is the main channel of Ca^{2+} efflux for liver tissue (Wingrove and Gunter, 1986). For the description of Ca^{2+} efflux through the $Ca^{2+}/2H^+$ exchanger (J_{CaH}) we used an empirical equation as given in (Wingrove and Gunter, 1986)

$$J_{CaH} = V_{\max}^{CaH} \frac{(Ca^{2+})^2}{(Ca^{2+})^2 + (k_m^{CaH})^2}, \quad (5)$$

where Ca^{2+} is concentration of free Ca^{2+} in matrix, and $V_{\max}^{CaH} = 1.2$ nmol Ca^{2+}/min/mg prot. and $k_m^{CaH} = 0.0084$ mM are taken from (Coll et al., 1982; Wingrove and Gunter, 1986). An additional pathway for Ca^{2+} efflux is provided by the opening of the PTP (Bernardi, 1999) (Module #5).

A.2.3. Intramitochondrial Ca^{2+} binding

Mitochondria can accumulate extremely large amounts of Ca^{2+} (Nicholls and Akerman, 1982), that binds to the matrix buffers, which are the membrane phospholipids (Reynafarje and Lehninger, 1969; Scarpa and Azzi, 1968) and anions of phosphate and oxidative substrates (Azzone et al., 1977; Reynafarje and Lehninger, 1969; Scarpa and Azzi, 1968). In system (12) below, we included these binding reactions and derived the Eq. (16) for the free matrix Ca^{2+} concentration.

A.3. Module #3. Mitochondrial potassium transport

A.3.1. K^+ channel (K^+ uniporter)

Available data suggests that K^+ influx, like that of Ca^{2+}, is driven by its electrophoretic uptake (Diwan and Tedeschi, 1975; Duchen, 1999; Jung et al., 1977). The dependence of the K^+ flux on the membrane potential could be approximated by Eiring's equation as was demonstrated in (Paucek et al., 1992):

$$J_K = P_K([K^+]_o \exp(\beta_K F\Delta\Psi/RT) - [K^+]_i \times \exp(-(1-\beta_K)F\Delta\Psi/RT), \quad (6)$$

where P_K is the membrane K^+ permeability; and $[K^+]_o$ and $[K^+]_i$ are extra- and intra-mitochondrial concentrations of K^+; $\beta_K = 0.25$ (Paucek et al., 1992). The P_K value of $P_K = 0.03$ µl/min/mg prot. accounts for the measured K^+ influx (30 nmol K^+/min/mg prot.) at high extra-mitochondrial K^+ concentration (Belyaeva and Wojtczak, 1994; Kowaltowski et al., 2001).

A.3.2. K/H exchanger

The fluxes of K^+ ions in mitochondria are best explained in terms of regulated interplay between the activity of a K^+ uniporter and a K/H exchanger (Chavez et al., 1977). We adopted the mechanism of the K/H exchanger described in (Chizmadzhev and Markin, 1974) as shown in Fig. 9. Here T_i, T_o, TH_i, TH_o, TK_i and TK_o are concentrations of the free and bound forms of the transporter at inner and outer sides of the membrane respectively (Chizmadzhev and Markin, 1974). K_H and K_K are the dissociation constants for complexes between the transporter and the H^+ and K^+, respectively. k is the rate of apparent diffusion of transporter across the membrane. The K/H flux is expressed as

$$J_{KH} = k(TK_i - TK_o). \quad (6a)$$

We assume that the rate of complex formation on both sides of the membrane is much faster then the diffusion of neutral complexes across the membrane, which allows us to express TK_i and TK_o:

$$TK_i = A_{Ki}T_i^{tot}; \quad TK_o = A_{Ko}T_o^{tot}, \quad (6b)$$

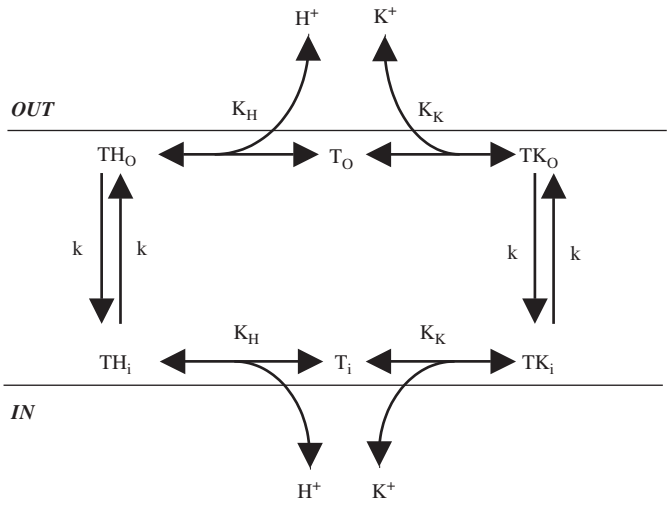

Fig. 9. The diagram of ion fluxes involved in electroneutral K^+/H^+ exchange across the membrane according (Chizmadzhev and Markin, 1974).

where the notations in Eq. 6(b) are defined as follows:

$$
\begin{aligned}
T_i^{tot} &= T_i + TH_i + TK_i;\\
T_o^{tot} &= T_o + TH_o + TK_o;\\
T^{total} &= T_i^{tot} + T_o^{tot};\\
T_i^{tot} &= \frac{T^{total}(A_{Ko} + A_{Ho})}{A_{Ko} + A_{Ho} + A_{Ki} + A_{Hi}};\\
A_{Ki} &= \frac{[K^+]_i}{K_K + \frac{K_K[H^+]_i}{K_H} + [K^+]_i};\\
A_{Ko} &= \frac{[K^+]_o}{K_K + \frac{K_K[H^+]_o}{K_H} + [K^+]_o};\\
A_{Hi} &= \frac{[H^+]_i}{K_H + \frac{K_H[K^+]_i}{K_K} + [H^+]_i};\\
A_{Ho} &= \frac{[H^+]_o}{K_H + \frac{K_H[K^+]_o}{K_K} + [H^+]_o}.
\end{aligned}
$$

Combining Eqs. (6a) and (6b) allows us to express the rate of electroneutral H^+/K^+ exchange across the mitochondrial inner membrane as

$$
J_{KH} = V_{\max}^{KH}\left(\frac{(A_{Ko} + A_{Ho})\cdot(A_{Ki} + A_{Ko})}{A_{Ko} + A_{Ho} + A_{Ki} + A_{Hi}} - A_{Ko}\right), \tag{7}
$$

where $[K^+]_o$, $[K^+]_i$, $[H^+]_o$, $[H^+]_i$, are internal "i" and external "o" concentrations of K^+ and H^+ ions, respectively. $V_{\max}^{KH}$ is the maximum rate of H^+/K^+ exchange that equals to 600 nmol H^+/min/mg prot., while $K_K = 40$ mM and $K_H = 1\times10^{-5}$ mM. Fig. 2C shows that with these constants the model describes well the experimentally observed dependence of the rate of the H^+/K^+ exchanger on the matrix pH and $[K^+]_o$ (Brierley and Jung, 1990).

A.4. Module #4. Mitochondrial anion transport

A.4.1. Electro-neutral P/OH exchanger

Inorganic phosphate enters the mitochondria via P/OH exchanger (Ligeti et al., 1985; Tyler and Sutton, 1984). The phosphate molecules are present in the form of mono (P^-) and double (P^{2-}) charged anions (Martell, 1964), and equilibrium in reactions occurring in the matrix and in the medium is determined by the pH of the matrix and medium correspondingly to dissociation reaction: $P^- \Leftrightarrow P^{2-} + H^+$. Assuming that P/OH exchanger is catalysed by the mechanism similar to that for K/H exchanger (Module #3), the following equation was developed for the rate of P^- uptake by mitochondria:

$$
\begin{aligned}
J_{POH} &= V_{\max}^{POH}\left(\frac{(A_{OHo} + A_{Po})(A_{OHi} + A_{OHo})}{A_{OHo} + A_{Po} + A_{OHi} + A_{Pi}} - A_{OHo}\right);\\
A_{OHi} &= \frac{[OH^-]_i}{K_{OH} + \frac{K_{OH}[P^-]_i}{K_P} + [OH^-]_i};\\
A_{OHo} &= \frac{[OH^-]_o}{K_{OH} + \frac{K_{OH}[P^-]_o}{K_P} + [OH^-]_o};\\
A_{Pi} &= \frac{[P^-]_i}{K_P + \frac{K_P[OH^-]_i}{K_{OH}} + [P^-]_i};\\
A_{Po} &= \frac{[P^-]_o}{K_P + \frac{K_P[OH^-]_o}{K_{OH}} + [P^-]_o};
\end{aligned}
\tag{8}
$$

where $[P^-]_o$, $[P^-]_i$, $[OH^-]_o$, $[OH^-]_i$, are internal "i" and external "o" concentrations of P^- and OH^- ions in mitochondria, respectively. The dissociation constants K_P, K_{OH} of the transporter and P^- and OH^- are $K_P = 1$ mM, $K_{OH} = 0.2$ μM, and the maximum rate of P/OH exchanger is $V_{\max}^{POH} = 7$ μmol/min/mg prot. The kinetic characteristics of the exchanger were defined from the experimental data on the kinetics of P^- transport in mitochondria incubated at 22 °C (Ligeti et al., 1985) (Fig. 2D). Phosphate flux through a membrane is temperature-dependent and its rate is sharply increasing upon the change in temperature from 22 to 37 °C (Ataullakhanov et al., 1978), resulting in increase of $V_{\max}^{POH}$ to 21 μmoles/min/mg prot. for experiments conducted at 37 °C.

A.4.2. Transport of oxidative substrates

Oxidative substrates enter the mitochondria either through specialized exchangers, which exchange of extramitochondrial species for matrix counter-ions, and/or by simple diffusion of the neutral molecules across the inner membrane (Tyler and Sutton, 1984). An estimate for a diffusion-mediated influx of 5 mM malate ($pK_1 = 3.5$, $pK_2 = 5.1$, $pH_{out} = 7.4$ (Martell, 1964)) into the mitochondria, with a surface area of $S\sim30\,cm^2$/mg prot. (Azzone and Massari, 1973) gives the value of <1 nmol malate/min/mg prot. (Stein, 1981). This influx of oxidative substrate is very small and cannot account for the actual rates of substrate anion (malate or succinate) uptake under an intensive influx of cations, which is around 100 nmol/min/

mg prot. (Evtodienko et al., 1980; Rossi et al., 1967). Thus, we assumed that the substrates of oxidation enter the matrix via a dicarboxylic acid exchanger (Tyler and Sutton, 1984). The equation for the substrate influx is

$$J_{dic} = V_{\max}^{dic}\left(A_{Po} - \frac{(A_{Po}+A_{Ao})(A_{Pi}+A_{Po})}{A_{Po}+A_{Ao}+A_{Pi}+A_{Ai}}\right);$$

$$A_{Pi} = \frac{[P^{2-}]_i}{K_P^{dic} + \frac{K_P^{dic}[A^{2-}]_i}{K_A} + [P^{2-}]_i};$$

$$A_{Po} = \frac{[P^{2-}]_o}{K_P^{dic} + \frac{K_P^{dic}[A^{2-}]_o}{K_A} + [P^{2-}]_o};$$

$$A_{Ai} = \frac{[A^{2-}]_i}{K_A + \frac{K_A[P^{2-}]_i}{K_P^{dic}} + [A^{2-}]_i};$$

$$A_{Ao} = \frac{[A^{2-}]_o}{K_A + \frac{K_A[P^{2-}]_o}{K_P^{dic}} + [A^{2-}]_o}; \quad (9)$$

where $[P^{2-}]_o$, $[P^{2-}]_i$, $[A^{2-}]_o$, $[A^{2-}]_i$, are the internal "i" and external "o" concentrations of P^{2-} and substrate ion (A^{2-}), respectively. K_P^{dic}, K_A- are the dissociation constants of the transporter and P^{2-} and A^{2-}, measured in Indiveri et al. (1989) and Tyler and Sutton (1984) (see Table 1). The rate of dicarboxylic acid exchange in mitochondria is comparable with the rate of the P/OH exchanger (Indiveri et al., 1989; Ligeti et al., 1985), therefore we assumed similarity in the maximum rates of these two processes (Table 1).

A.5. Module #5. Mitochondrial permeability transition pore

A.5.1. Regulation of the mitochondrial permeability transition pore

PTP has been suggested to provide an important pathway of Ca^{2+} release (Bernardi, 1999; Duchen, 1999). PTP is activated by many factors, such as matrix swelling (Holmuhamedov et al., 1999; Lemasters et al., 1999), oxidative stress (Catisti and Vercesi, 1999; Petronilli et al., 1993), and Ca^{2+}-overload, which is the main activator (Bernardi, 1999; Duchen, 1999; Hunter and Haworth, 1979). The rate of PTP activation is dependent on the actual Ca^{2+} load and mitochondrial membrane potential ($\Delta\Psi$) (Petronilli et al., 1993), and is inhibited by acidic pH_{in} (Szabo et al., 1992). Using an approach developed in our paper (Selivanov et al., 1998), and experimental data (Hunter and Haworth, 1979; Petronilli et al., 1993; Szabo et al., 1992), the following equation, describing the opening and closure of the PTP, we obtained

$$\frac{dT_{op}}{dt} = k_{op}\, Ca^{2+} p(\Delta\Psi)(1 - T_{op}) - k_{cl}\, T_{op}\frac{H^+}{H^+ + k_m^{PTP}}, \quad (10)$$

where T_{op} and $(1-T_{op})$ are the relative numbers of "open" and "closed" pores (Selivanov et al., 1998). The dependence of the PTP opening rate on the mitochondrial membrane potential $p(\Delta\Psi)$ was estimated from experimental data (Petronilli et al., 1993) as

$$p(\Delta\Psi) = \begin{bmatrix} \exp((\Psi_0 - \Delta\Psi)/\Psi_1); & \Delta\Psi > \Psi_2, \\ \exp((\Psi_0 - \Psi_2)/\Psi_1); & \Delta\Psi < \Psi_2, \end{bmatrix}$$

where k_m^{PTP} taken as 3.2×10^{-5} mM (Szabo et al., 1992), $\Psi_0 = 110$ mV, $\Psi_1 = 20$ mV, $\Psi_2 = 70$ mV, $k_{op} = 2\,\text{min}^{-1}$, and $k_{cl} = 100\,\text{min}^{-1}$ (Evtodienko et al., 1980; Petronilli et al., 1993). Fig. 2E shows that with these constants the model describes well the experimentally observed dependence of the PTP opening rate on the membrane potential.

A.5.2. Ion fluxes through non-specific PTP

The equation, describing ion fluxes through PTP is given as follows (Selivanov et al., 1998):

$$L = P_{PTP} T_{op} z \frac{F\Delta\Psi}{RT}\frac{C_{in}\exp\left(-z\frac{F\Delta\Psi}{RT}\right) - C_{out}}{1 - \exp\left(-z\frac{F\Delta\Psi}{RT}\right)}, \quad (11)$$

where C_{in} and C_{out} are the intra- and extra-mitochondrial ion concentrations; P_{PTP} is the ion permeability of the pore. P_{PTP} was estimated using experimental data (Evtodienko et al., 1980) as 30 μl/mg prot./min for anions (P_{PTP}^a) and 3 μl/mg prot./min for cations (P_{PTP}^c). The flux of neutral molecules ($[Ca{-}P]$ and $[Ca{-}A]$) through PTP follows Fick's diffusion law (Stein, 1981):

$$L = P_{PTP}^n (C_{in} - C_{out}),$$

where P_{PTP}^n was estimated as 100 μl/mg prot./min (Evtodienko et al., 1980).

A.5.3. Complete mathematical model of mitochondrial ion transport

The following system of ordinary differential equations describes the mathematical model of ion fluxes across the inner mitochondrial membrane (Fig. 1):

$$\frac{d(Ca_t^{2+})}{dt} = J_{uni} - J_{CaH} - L_{Ca} - k_{-1,CaP} v P^{2-} Ca^{2+} + k_{1,CaP} v [Ca-P],$$

$$\frac{d(H_t^+)}{dt} = -J_{H,res} + J_{H,leak} - L_H + J_{POH} + J_{KH} + J_{CaH}2 + k_{1,p} v P^- - k_{-1,p} v P^{2-} H^+,$$

$$\frac{d(P_t^-)}{dt} = J_{POH} - k_{1,p} v P^- + k_{-1,p} v P^{2-} H^+ - L_{P^-},$$

$$\frac{d(P_t^{2-})}{dt} = J_{dic} + k_{1,p} v P^- - k_{-1,p} v P^{2-} H^+ - k_{-1,CaP} v P^{2-} Ca^{2+} + k_{1,CaP} v [Ca-P] - L_{P^{2-}},$$

$$\frac{d(A_t^{2-})}{dt} = J_{dic} - k_{-1,CaA} v A^{2-} Ca^{2+} + k_{1,CaA} v [Ca-A] - L_A,$$

$$\frac{d(K_t^+)}{dt} = J_K - L_K - J_{KH},$$

$$\begin{aligned}
\frac{d([Ca-P]_t)}{dt} &= -L_{Ca-P} + k_{-1,CaP} v P^{2-} Ca^{2+} \\
&\quad - k_{1,CaP} v [Ca-P], \\
\frac{d([Ca-A]_t)}{dt} &= -L_{Ca-A} + k_{-1,CaA} v A^{2-} Ca^{2+} \\
&\quad - k_{1,CaA} v [Ca-A], \\
\frac{d([Ca-PL]_t)}{dt} &= k_{-1,CaPL} v PL^{2-} Ca^{2+} \\
&\quad - k_{1,CaPL} v [Ca-PL], \\
\frac{d(NAD_t^+)}{dt} &= J_{H,res}/12 - J_{NADH},
\end{aligned} \tag{12}$$

where $Ca_t{}^{2+}$, $H_t{}^+$, $K_t{}^+$, $P_t{}^-$, $P_t{}^{2-}$, $NAD_t{}^+$, $A_t{}^{2-}$, $PL_t{}^{2-}$ are the matrix amount of free Ca^{2+}, H^+, K^+, P^-, P^{2-}, NAD^+, substrate A^{2-} and membrane phospholipids PL^{2-}. $[Ca{-}P]_t$, $[Ca{-}A]_t$, $[Ca{-}PL]_t$, are the matrix content of Ca^{2+} complexes with P^{2-}, substrate (A^{2-}) and PL^{2-}, respectively. The same symbols without a subscript "t" represent the ion concentrations determined by dividing the value of the matrix content by the matrix volume (v). The entire amount of each species was kept constant.

The membrane potential is determined by all electrogenic fluxes as follows [25]:

$$\begin{aligned}
C_{mito}\frac{d(\Delta\Psi)}{dt} &= (J_{H,res} - J_{H,leak}, \\
&\quad + 2(L_{Ca} - L_{P^{2-}} - L_A - J_{uni}) \\
&\quad + L_K - J_K - L_{P^-} + L_H),
\end{aligned} \tag{13}$$

where C_{mito} is the electrical capacitance of the mitochondrial membrane taken as 1.45×10^{-3} nmol/mV/mg prot. (Magnus and Keizer, 1997, 1998).

The system of differential Eq. (12) could be reduced using the fact that the rates of Ca binding to the buffers and dissociation of inorganic phosphate are considerably higher then the rates of ion translocation across the membrane (Kuznetzov, 1995). The reduced system of differential equations is

$$\begin{aligned}
\frac{d(Ca)}{dt} &= J_{uni} - J_{CaH} - L_{Ca} - L_{Ca-P} - L_{Ca-A}, \\
C_{mito}\frac{d(\Delta\Psi)}{dt} &= (J_{H,res} - J_{H,leak} \\
&\quad + 2(L_{Ca} - L_{P^{2-}} - L_A - J_{uni}) \\
&\quad + L_K - J_K - L_{P^-} + L_H), \\
\frac{d(H)}{dt} &= -J_{H,res} + J_{H,leak} - L_H + 2J_{POH} \\
&\quad + J_{KH} + J_{CaH}2 - L_{P^-}, \\
\frac{d(P)}{dt} &= J_{POH} - J_{dic} - L_{Ca-P} - L_{P^-} - L_{P^{2-}}, \\
\frac{d(A)}{dt} &= J_{dic} - L_{Ca-A} - L_A, \\
\frac{d(K)}{dt} &= J_K - L_K - J_{KH}, \\
\frac{d(NAD)}{dt} &= J_{H,res}/12 - J_{NADH},
\end{aligned} \tag{14}$$

with the new variables:

$$\begin{aligned}
Ca &= Ca_t^{2+} + [Ca-P]_t + [Ca-PL]_t + [Ca-A]_t, \\
A &= A_t^{2-} + [Ca-A]_t, \\
P &= P_t^{2-} + P_t^{-} + [Ca-P]_t, \\
H &= H_t^{+} + P_t^{-}, \\
NAD &= NAD_t^{+}, \\
K &= K_t^{+}.
\end{aligned}$$

Using the equilibrium condition for dissociation of inorganic phosphate and Ca^{2+} complexes with anions we express the concentrations of Ca^{2+} complexes and P^{2-} as

$$\begin{aligned}
[Ca-PL]_t &= PL_t^0\, Ca^{2+}/(k_d^{Ca-PL} + Ca^{2+}), \\
[Ca-A]_t &= A\, Ca^{2+}/(k_d^{Ca-A} + Ca^{2+}), \\
[Ca-P]_t &= P\, Ca^{2+}/(k_d^{Ca-P}(1 + H^+/k_d^P + Ca^{2+}/k_d^{Ca-P})), \\
P_t^{2-} &= P/(1 + H^+/k_d^P + Ca^{2+}/k_d^{Ca-P}),
\end{aligned} \tag{15}$$

where $PL_t{}^0$ is the total amount of phospholipids. The dissociation constants for phosphate and complexes of Ca^{2+} with anions (PL^{2-}, P^{2-}, A^{2-}) were taken as $k_d^P = 6\times10^{-5}$ mM (Martell, 1964); $k_d^{Ca-PL} = 0.023$ mM (Hansford and Castro, 1982; Scarpa and Azzi, 1968), $k_d^{Ca-A} = k_d^{Ca-P} = 3$ mM (Martell, 1964). $PL_t{}^0 = 40$ nmol/mg prot. (Scarpa and Azzi, 1968).

Mitochondria accumulating Ca^{2+} and K^+ ions are characterized by an alkaline matrix (Nicholls and Akerman, 1982), therefore the term $H^+/k_d{}^P$ in the Eq. (15) for $[Ca{-}P]_t$ can be neglected ($k_d{}^P = 0.06\,\mu$M), allowing to derive and solve cubic equation for the free matrix Ca^{2+} concentration. We expressed the free matrix Ca^{2+} analytically as a function of the total matrix Ca^{2+}, oxidative substrates, phosphate and phospholipids:

$$Ca^{2+} = \sqrt{\frac{4p}{3}}\cos\left(\frac{\pi}{3} - arc\cos\left(\frac{q}{2}\left(\frac{3}{p}\right)^{3/2}\right)\Big/3\right) - b/3,$$

where

$$\begin{aligned}
&p = b^2/3 - c; \quad q = 2b^3/27 - bc/3 - d; \\
&b = k_d^{Ca-P} + k_d^{Ca-PL} + (PL_t^0 + P + A - Ca)/v; \\
&d = k_d^{Ca-P} k_d^{Ca-PL} Ca/v; \\
&c = k_d^{Ca-P} k_d^{Ca-PL} \\
&\quad + [PL_t^0 k_d^{Ca-P} + (P+A)k_d^{Ca-PL} - Ca(k_d^{Ca-P} + k_d^{Ca-PL})]/v.
\end{aligned} \tag{16}$$

The mitochondrial volume v is proportional to the matrix content of osmotically active substances and can be defined as follows (Beavis et al., 1985):

$$v = v_0 + (K + P + A + Ca^{2+} + S_0)/F, \tag{17}$$

where v_0 is the osmotically inactive volume, S_0 is the matrix solute content, and F—the external osmolarity. Constants were taken from experimental data (Beavis et al., 1985) as $S_0 = 87$ nmol/mg prot., $v_0 = 0.28\,\mu$l/mg prot.

A.6. Glossary and units

The values of all variables in the system of ODEs (14), such as matrix content of Ca^{2+}, H^+, phosphate, substrate anion, K^+, NAD^+ are expressed in nmol/mg prot., while intra- and extra-mitochondrial concentrations are expressed in mM; mitochondrial membrane potential is expressed in mV and the rate of translocation of participating species across the inner mitochondrial membrane is expressed in nmol/mg prot./min. These rates are:

J_{uni}—the rate of Ca^{2+} flux via a mitochondrial Ca^{2+} uniporter;
J_{CaH}—the rate of Ca^{2+} and/or H^+ fluxes via an electroneutral Ca/2H exchanger;
$J_{H,res}$—the rate of H^+ flux via the respiratory chain, supported by NADH oxidation;
$J_{H,leak}$—the rate of back-flow of H^+ ions via "leakage" of the mitochondrial membrane;
J_K—the rate of K^+ flux via the mitochondrial K^+ uniporter;
J_{KH}—the rate of K^+ and/or H^+ fluxes via an electroneutral K/H exchanger;
J_{POH}—the rate of inorganic phosphate flux via a mitochondrial P/OH exchanger;
J_{dic}—the rate of P^{2-} and A^{2-} fluxes via a mitochondrial dicarboxylic acid exchanger;
J_{NADH}—the rate of NADH recovery from NAD by matrix dehydrogenases;
L_{Ca}, L_{Ca-P}, L_{Ca-A}, L_A, L_K, L_{P^-}, $L_{P^{2-}}$, L_H—the rates of corresponding ion fluxes via PTP.

References

Ataullakhanov, F.I., Vitvitskii, V.M., Platonova, O.V., 1978. Human erythrocyte membrane permeability for arsenate and formation of trivalent arsenic compounds. Biofizika 23, 1101–1103.

Azzone, G.F., Massari, S., 1973. Active transport and binding in mitochondria. Biochim. Biophys. Acta 301, 195–226.

Azzone, G.F., Bragadin, M., Pozzan, T., Antone, P.D., 1977. Proton electrochemical potential in steady state rat liver mitochondria. Biochim. Biophys. Acta 459, 96–109.

Beavis, A.D., Brannan, R.D., Garlid, K.D., 1985. Swelling and contraction of the mitochondrial matrix, I: a structural interpretation of the relationship between light scattering and matrix volume. J. Biol. Chem. 260, 13424–13433.

Belyaeva, E.A., Wojtczak, L., 1994. An attempt to quantify K^+ fluxes in rat liver mitochondria. Biochem. Mol. Biol. Int. 33, 165–175.

Bernardi, P., 1999. Mitochondrial transport of cations: channels, exchangers, and permeability transition. Physiol. Rev. 79, 1127–1155.

Berridge, M.J., Bootman, M.D., Roderick, H.L., 2003. Calcium signalling: dynamics, homeostasis and remodelling. Nat. Rev. Mol. Cell Biol. 4, 517–529.

Bowser, D.N., Petrou, S., Panchal, R.G., Smart, M.L., Williams, D.A., 2002. Release of mitochondrial Ca^{2+} via the permeability transition activates endoplasmic reticulum Ca^{2+} uptake. FASEB J. 16, 1105–1107.

Brierley, G.P., Jung, D.W., 1990. Kinetic properties of the K^+/H^+ antiport of heart mitochondria. Biochemistry 29, 408–415.

Brown, G.C., Brand, M.D., 1986. Changes in permeability to protons and other cations at high proton motive force in rat liver mitochondria. Biochem. J. 234, 75–81.

Buckman, J.F., Reynolds, I.J., 2001. Spontaneous changes in mitochondrial membrane potential in cultured neurons. J. Neurosci. 21, 5054–5065.

Carafoli, E., Gamble, R.L., Lehninger, A.L., 1965. K^+-dependent rebounds and oscillations in respiration-linked movements of Ca^{++} and H^+ in rat liver mitochondria. Biochem. Biophys. Res. Commun. 21, 488–493.

Catisti, R., Vercesi, A.E., 1999. The participation of pyridine nucleotides redox state and reactive oxygen in the fatty acid-induced permeability transition in rat liver mitochondria. FEBS Lett. 464, 97–101.

Chance, B., 1965. The energy-linked reaction of calcium with mitochondria. J. Biol. Chem. 240, 2729–2748.

Chance, B., Yoshioka, T., 1966. Sustained oscillations of ionic constituents of mitochondria. Arch. Biochem. Biophys. 117, 451–465.

Chavez, E., Jung, D.W., Brierley, G.P., 1977. Energy-dependent efflux of K^+ from heart mitochondria. Biochem. Biophys. Res. Commun. 75, 69–75.

Chizmadzhev, Iu.A., Markin, V.S., 1974. Mobile transporters. In: Induced Ion Transport. Science Press, Moscow.

Coll, K.E., Joseph, S.K., Corkey, B.E., Williamson, J.R., 1982. Determination of the matrix free Ca^{2+} concentration and kinetics of Ca^{2+} efflux in liver and heart mitochondria. J. Biol. Chem. 257, 8696–8704.

Collins, T.J., Berridge, M.J., Lipp, P., Bootman, M.D., 2002. Mitochondria are morphologically and functionally heterogeneous within cells. EMBO J. 21, 1616–1627.

Cortassa, S., Aon, M.A., Marban, E., Winslow, R.L., O'Rourke, B., 2003. An integrated model of cardiac mitochondrial energy metabolism and calcium dynamics. Biophys. J. 84, 2734–2755.

Diwan, J.J., Tedeschi, H., 1975. K+ fluxes and the mitochondrial membrane potential. FEBS Lett. 60, 176–179.

Doussiere, J., Ligeti, E., Brandolin, G., Vignais, P.V., 1984. Control of oxidative phosphorylation in rat heart mitochondria. The role of the adenine nucleotide carrier. Biochim. Biophys. Acta 766, 492–500.

Duchen, M.R., 1999. Contributions of mitochondria to animal physiology: from homeostatic sensor to calcium signalling and cell death. J. Physiol. 516 (Part 1), 1–17.

Erecinska, M., Wilson, D.F., 1982. Regulation of cellular energy metabolism. J. Membr. Biol. 70, 1–14.

Eriksson, O., Pollesello, P., Geimonen, E., 1999. Regulation of total mitochondrial Ca^{2+} in perfused liver is independent of the permeability transition pore. Am. J. Physiol. 276, C1297–C1302.

Evtodienko, Y.V., Zinchenko, V.P., Holmuhamedov, E.L., Gylkhandanyan, A.V., Zhabotinsky, A.M., 1980. The stoichiometry of ion fluxes during Sr^{2+}-induced oscillations in mitochondria. Biochim. Biophys. Acta 589, 157–161.

Falcke, M., Hudson, J.L., Camacho, P., Lechleiter, J.D., 1999. Impact of mitochondrial Ca^{2+} cycling on pattern formation and stability. Biophys. J. 77, 37–44.

Fuller, K.M., Arriaga, E.A., 2003. Advances in the analysis of single mitochondria. Curr. Opin. Biotechnol. 14, 35–41.

Garlid, K.D., Beavis, A.D., Ratkje, S.K., 1989. On the nature of ion leaks in energy-transducing membranes. Biochim. Biophys. Acta 976, 109–120.

Gooch, V.D., Packer, L., 1974. Oscillatory systems in mitochondria. Biochim. Biophys. Acta 346, 245–260.

Goryanin, I., Hodgman, T.C., Selkov, E., 1999. Mathematical simulation and analysis of cellular metabolism and regulation. Bioinformatics 15, 749–758.

Graven, S.N., Lardy, H.A., Rutter, A., 1966. Antibiotics as tools for metabolic studies, VI: damped oscillatory swelling of mitochondria induced by nonactin, monactin, dinactin, and trinactin. Biochemistry 5, 1735–1742.

Gunter, T.E., Pfeiffer, D.R., 1990. Mechanisms by which mitochondria transport calcium. Am. J. Physiol 258, C755–C786.

Gunter, T.E., Yule, D.I., Gunter, K.K., Eliseev, R.A., Salter, J.D., 2004. Calcium and mitochondria. FEBS Lett. 567, 96–102.

Hansford, R.G., Castro, F., 1982. Intramitochondrial and extramitochondrial free calcium ion concentrations of suspensions of heart mitochondria with very low, plausibly physiological, contents of total calcium. J. Bioenerg. Biomembr. 14, 361–376.

Herrington, J., Park, Y.B., Babcock, D.F., Hille, B., 1996. Dominant role of mitochondria in clearance of large Ca^{2+} loads from rat adrenal chromaffin cells. Neuron 16, 219–228.

Hindmarsh, A.C., 1980. LSODE and LSODI, two new initial value ordinary differential equation solvers. ACM-Signum Newslett. 15, 10–11.

Holmuhamedov, E.L., 1986. Oscillating dissipative structures in mitochondrial suspensions. Eur. J. Biochem. 158, 543–546.

Holmuhamedov, E.L., Teplova, V.V., Chukhlova, E.A., Evtodienko, Y.V., Ulrich, R.G., 1995. Strontium excitability of the inner mitochondrial membrane: regenerative strontium-induced strontium release. Biochem. Mol. Biol. Int. 36, 39–49.

Holmuhamedov, E.L., Wang, L., Terzic, A., 1999. ATP-sensitive K^+ channel openers prevent Ca^{2+} overload in rat cardiac mitochondria. J. Physiol. 519 (Part 2), 347–360.

Holzhutter, H.G., Henke, W., Dubiel, W., Gerber, G., 1985. A mathematical model to study short-term regulation of mitochondrial energy transduction. Biochim. Biophys. Acta 810, 252–268.

Hoth, M., Fanger, C.M., Lewis, R.S., 1997. Mitochondrial regulation of store-operated calcium signaling in T lymphocytes. J. Cell Biol. 137, 633–648.

Hoth, M., Button, D.C., Lewis, R.S., 2000. Mitochondrial control of calcium-channel gating: a mechanism for sustained signaling and transcriptional activation in T lymphocytes. Proc. Natl. Acad. Sci. USA 97, 10607–10612.

Hunter, D.R., Haworth, R.A., 1979. The Ca^{2+}-induced membrane transition in mitochondria, I: the protective mechanisms. Arch. Biochem. Biophys. 195, 453–459.

Huser, J., Blatter, L.A., 1999. Fluctuations in mitochondrial membrane potential caused by repetitive gating of the permeability transition pore. Biochem. J. 343 (Part 2), 311–317.

Ichas, F., Jouaville, L.S., Sidash, S.S., Mazat, J.P., Holmuhamedov, E.L., 1994. Mitochondrial calcium spiking: a transduction mechanism based on calcium-induced permeability transition involved in cell calcium signalling. FEBS Lett. 348, 211–215.

Indiveri, C., Capobianco, L., Kramer, R., Palmieri, F., 1989. Kinetics of the reconstituted dicarboxylate carrier from rat liver mitochondria. Biochim. Biophys. Acta 977, 187–193.

Jouaville, L.S., Ichas, F., Holmuhamedov, E.L., Camacho, P., Lechleiter, J.D., 1995. Synchronization of calcium waves by mitochondrial substrates in Xenopus laevis oocytes. Nature 377, 438–441.

Jung, D.W., Chavez, E., Brierley, G.P., 1977. Energy-dependent exchange of K^+ in heart mitochondria K^+ influx. Arch. Biochem. Biophys. 183, 452–459.

Jung, D.W., Davis, M.H., Brierley, G.P., 1989. Estimation of matrix pH in isolated heart mitochondria using a fluorescent probe. Anal. Biochem. 178, 348–354.

Kapus, A., Szaszi, K., Kaldi, K., Ligeti, E., Fonyo, A., 1991. Is the mitochondrial Ca^{2+} uniporter a voltage-modulated transport pathway? FEBS Lett. 282, 61–64.

Kauffman, R.F., Lardy, H.A., 1980. Biphasic uptake of Ca^{2+} by rat liver mitochondria. J. Biol. Chem. 255, 4228–4235.

Kowaltowski, A.J., Seetharaman, S., Paucek, P., Garlid, K.D., 2001. Bioenergetic consequences of opening the ATP-sensitive K(+) channel of heart mitochondria. Am. J. Physiol. Heart Circ. Physiol. 280, H649–H657.

Kroemer, G., Martin, S.J., 2005. Caspase-independent cell death. Nat. Med. 11, 725–730.

Kuznetzov, Y., 1995. Elements of Applied Bifurcation Theory. Springer, New York.

Lemasters, J.J., Qian, T., Bradham, C.A., Brenner, D.A., Cascio, W.E., Trost, L.C., Nishimura, Y., Nieminen, A.L., Herman, B., 1999. Mitochondrial dysfunction in the pathogenesis of necrotic and apoptotic cell death. J. Bioenerg. Biomembr. 31, 305–319.

Ligeti, E., Brandolin, G., Dupont, Y., Vignais, P.V., 1985. Kinetics of Pi–Pi exchange in rat liver mitochondria: rapid filtration experiments in the millisecond time range. Biochemistry 24, 4423–4428.

Lin, X., Varnai, P., Csordas, G., Balla, A., Nagai, T., Miyawaki, A., Balla, T., Hajnoczky, G., 2005. Control of calcium signal propagation to the mitochondria by inositol 1,4,5-trisphosphate-binding proteins. J. Biol. Chem. 280, 12820–12832.

Magnus, G., Keizer, J., 1997. Minimal model of beta-cell mitochondrial Ca^{2+} handling. Am. J. Physiol. 273, C717–C733.

Magnus, G., Keizer, J., 1998. Model of beta-cell mitochondrial calcium handling and electrical activity, II: mitochondrial variables. Am. J. Physiol. 274, C1174–C1184.

Marhl, M., Haberichter, T., Brumen, M., Heinrich, R., 2000. Complex calcium oscillations and the role of mitochondria and cytosolic proteins. Biosystems 57, 75–86.

Martell, A.E., 1964. Stability constants of metal–ion complexes. In: Organic Ligands. The Chemical Society, pp. 330–370.

McCormack, J.G., Denton, R.M., 1993. The role of intramitochondrial Ca^{2+} in the regulation of oxidative phosphorylation in mammalian tissues. Biochem. Soc. Trans. 21 (Part 3), 793–799.

Meyer, T., Stryer, L., 1988. Molecular model for receptor-stimulated calcium spiking. Proc. Natl Acad. Sci. USA 85, 5051–5055.

Mitchell, P., 1972. Chemiosmotic coupling in energy transduction: a logical development of biochemical knowledge. J. Bioenerg. 3, 5–24.

Mitchell, P., Moyle, J., 1969. Estimation of membrane potential and pH difference across the cristae membrane of rat liver mitochondria. Eur. J. Biochem. 7, 471–484.

Monteith, G.R., Blaustein, M.P., 1999. Heterogeneity of mitochondrial matrix free Ca^{2+}: resolution of Ca^{2+} dynamics in individual mitochondria in situ. Am. J. Physiol. 276, C1193–C1204.

Nicholls, D., Akerman, K., 1982. Mitochondrial calcium transport. Biochim. Biophys. Acta 683, 57–88.

Parekh, A.B., Putney Jr., J.W., 2005. Store-operated calcium channels. Physiol. Rev. 85, 757–810.

Paucek, P., Mironova, G., Mahdi, F., Beavis, A.D., Woldegiorgis, G., Garlid, K.D., 1992. Reconstitution and partial purification of the glibenclamide-sensitive, ATP-dependent K^+ channel from rat liver and beef heart mitochondria. J. Biol. Chem. 267, 26062–26069.

Petronilli, V., Cola, C., Massari, S., Colonna, R., Bernardi, P., 1993. Physiological effectors modify voltage sensing by the cyclosporin A-sensitive permeability transition pore of mitochondria. J. Biol. Chem. 268, 21939–21945.

Pietrobon, D., Caplan, S.R., 1985. Flow-force relationships for a six-state proton pump model: intrinsic uncoupling, kinetic equivalence of input and output forces, and domain of approximate linearity. Biochemistry 24, 5764–5776.

Reynafarje, B., Lehninger, A.L., 1969. High affinity and low affinity binding of Ca++ by rat liver mitochondria. J. Biol. Chem. 244, 584–593.

Rizzuto, R., Pozzan, T., 2006. Microdomains of intracellular Ca^{2+}: molecular determinants and functional consequences. Physiol. Rev. 86, 369–408.

Robb-Gaspers, L.D., Rutter, G.A., Burnett, P., Hajnoczky, G., Denton, R.M., Thomas, A.P., 1998. Coupling between cytosolic and mitochondrial calcium oscillations: role in the regulation of hepatic metabolism. Biochim. Biophys. Acta 1366, 17–32.

Rossi, C., Scarpa, A., Azzone, G.F., 1967. Ion transport in liver mitochondria, V: the effect of anions on the mechanism of aerobic K^+ uptake. Biochemistry 6, 3902–3910.

Rudolf, R., Mongillo, M., Magalhaes, P.J., Pozzan, T., 2004. In vivo monitoring of Ca(2+) uptake into mitochondria of mouse skeletal muscle during contraction. J. Cell Biol. 166, 527–536.

Scarpa, A., Azzi, A., 1968. Cation binding to submitochondrial particles. Biochim. Biophys. Acta 150, 473–481.

Selivanov, V.A., Ichas, F., Holmuhamedov, E.L., Jouaville, L.S., Evtodienko, Y.V., Mazat, J.P., 1998. A model of mitochondrial Ca(2+)-induced Ca^{2+} release simulating the Ca^{2+} oscillations and spikes generated by mitochondria. Biophys. Chem. 72, 111–121.

Stein, W.D., 1981. Permeability for lipophilic molecules. In: Bonting, S.L., de Pont, J.J.H.H.M. (Eds.), Membrane Transport. Elsevier, Amsterdam, pp. 1–28.

Szabo, I., Bernardi, P., Zoratti, M., 1992. Modulation of the mitochondrial megachannel by divalent cations and protons. J. Biol. Chem. 267, 2940–2946.

Tashmukhamedov, B.A., Gagel'gans, A.I., 1970. Oscillatory nature of H^+ yield from mitochondria during strontium accumulation. Biofizika 15, 443–446.

Tyler, D.D., Sutton, C.M., 1984. Mitochondrial transporting systems. In: Bitter, E.E. (Ed.), Membrane Structure and Function, pp. 182–270.

Wingrove, D.E., Gunter, T.E., 1986. Kinetics of mitochondrial calcium transport, I: characteristics of the sodium-independent calcium efflux mechanism of liver mitochondria. J. Biol. Chem. 261, 15159–15165.

Wingrove, D.E., Amatruda, J.M., Gunter, T.E., 1984. Glucagon effects on the membrane potential and calcium uptake rate of rat liver mitochondria. J. Biol. Chem. 259, 9390–9394.